Facially Coordinating Cyclic Triamines, Part 1

The Coordination Chemistry of *cis*-3,5-Diaminopiperidine and Substituted Derivatives

Jörg W. Pauly,[a] Jürgen Sander,[a] Dirk Kuppert,[a] Manuela Winter,[b] Guido J. Reiss,[c] Fabio Zürcher,[d] Rudolf Hoffmann,[d] Thomas F. Fässler,[d] and Kaspar Hegetschweiler*[a]

Abstract: An efficient and convenient method for the preparation of *cis*-3,5-diaminopiperidine (dapi) has been established and the coordination chemistry of this ligand with Co^{II}, Co^{III}, Ni^{II}, Cu^{II}, Zn^{II}, and Cd^{II} has been investigated in the solid state and in aqueous solution. Potentiometric measurements revealed a generally high stability for the bis complexes of the divalent cations with maximum stability for Ni^{II} ($\log \beta_2 = 21.2$, $\beta_2 = [M(dapi)_2][M]^{-1}[dapi]^{-2}$, 25 °C, $\mu = 0.1$ mol dm^{-3}). Cyclic voltammetry established quasi-reversible formation of $[Ni(dapi)_2]^{3+}$ with a redox potential of 0.91 V (versus NHE) for the $Ni^{II/III}$ couple. $[Co(dapi)_2]^{3+}$ was prepared by aerial oxidation of the corresponding Co^{II} precursor. The two isomers *trans*-$[Co(dapi)_2]^{3+}$ (**1**$^{3+}$, 26%) and *cis*-$[Co(dapi)_2]^{3+}$ (**2**$^{3+}$, 74%), have been separated and isolated as solid Cl^- and $CF_3SO_3^-$ salts. In a non-aqueous medium **1**$^{3+}$ and **2**$^{3+}$ reacted with paraformaldehyde and NEt_3 to give the methylidene-imino derivatives **3**$^{3+}$ and **4**$^{3+}$, in which the two piperidine rings are bridged by two or one N-CH_2-O-CH_2-N bridges, respectively. Crystal structure analyses were performed for H_3dapi[$ZnCl_4$]Cl, **1**$Cl_3 \cdot 2H_2O$, **2**$Cl_3 \cdot H_2O$, **3**[$ZnCl_4$]Cl, **4**[$ZnCl_4$]Cl, $[Ni(dapi)_2]Cl_2 \cdot H_2O$, $[Cu(dapi)_2](NO_3)_2$, $[Cu(dapi)Cl_2]$, $[(dapi)ClCd\text{-}(\mu_2\text{-}Cl)_2\text{-}CdCl(dapi)]$, and $[Co(dapi)(NO_2)(CO_3)]$. The stability of $[M^{II}(dapi)]^{2+}$ and $[M^{II}(dapi)_2]^{2+}$ complexes in aqueous solution, particularly the remarkably high tendency of $[M(dapi)]^{2+}$ to undergo coordinative disproportionation is discussed in terms of the specific steric requirements of this ligand. Molecular mechanics calculations have been performed to analyze the different types of strain in these complexes. A variety of alkylated derivatives of dapi have been prepared by reductive alkylation with formaldehyde, benzaldehyde, salicylaldehyde, and pyridine-2-carbaldehyde. The Ni^{II} complexes of the pentadentate N^3,N^5-bis-(2-pyridinylmethyl)-*cis*-3,5-diaminopiperidine (py_2dapi) and the hexadentate N^3,N^5,1-tris(2-pyridinylmethyl)-*cis*-3,5-diaminopiperidine (py_3dapi) have been isolated as crystalline ClO_4^- salts [Ni(py_2dapi)Cl]ClO_4 and [Ni(py_3dapi)]$(ClO_4)_2 \cdot H_2O$ and characterized by crystal structure analyses.

Keywords: N ligands · polyamines · stability constants · structure elucidation

Introduction

The metal binding properties of aliphatic polyamines have been well known for many years.[1] Along with aliphatic polyamino-polycarboxylates, this class of compounds probably constitutes the most extensively investigated group of chelating agents. Several different factors influence the stability of the complexes formed; these include the number of donor atoms, the specific steric requirements of the ligand backbone, the nature of the metal center, and solvation effects.[2] For open chain ligands, the assignment of the correct solution structure, as required for a conclusive structure–stability correlation, is often a difficult task. A variety of isomers have to be accounted for, and steric strain within the ligand backbone may frequently result in partial coordination of the donor set. This has been pointed out, for instance, for the potentially hexadentate ethylenedinitrilotetrakis(ethyleneamine), which exhibited pentadentate coordination in its

[a] Prof. K. Hegetschweiler, Dipl.-Chem. J. W. Pauly, Dipl.-Chem. J. Sander, Dipl.-Chem. D. Kuppert
Anorganische Chemie, Universität des Saarlandes
Postfach 15 11 50, 66041 Saarbrücken (Germany)
Fax: (+49) 681-302-2663
E-mail: hegetsch@mx.uni-saarland.de

[b] M. Winter
Analytische Chemie, Ruhr-Universität
Universitätsstrasse 150, 44780 Bochum (Germany)

[c] Dr. G. J. Reiss
Institut für Anorganische Chemie und Strukturchemie
Heinrich Heine Universität Düsseldorf, Universitätsstrasse 1
40225 Düsseldorf (Germany)

[d] Dr. F. Zürcher, Dr. R. Hoffmann, Prof. T. F. Fässler
Laboratorium für Anorganische Chemie, ETH-Zentrum
8092 Zürich (Switzerland)

Supporting information for this article is available on the WWW under http://www.wiley-vch.de/home/chemistry/ or from the author. Tables S1–S3 list ^{1}H NMR data of $H_x$dapi^{x+} (chemical shifts, deshielding constants) and Tables S4–S6 list potentiometric data for the determination of equilibrium constants.

  0947-6539/00/0615-2830 $ 17.50+.50/0

Zn^{II} and Cu^{II} complexes,[3] and for the potentially tridentate 1,2,3-propanetriamine, for which a bidentate coordination has been found for Cu^{II}.[4] This problem is particularly significant in labile systems involving flexible chain ligands, where rapid equilibrium between the different forms must be taken into consideration.

For the more sterically constrained, cyclic polyamines, structure–stability correlations are more readily obtained because the potential for different types of metal–ligand interactions is considerably reduced. In fact, the tetraaza macrocycles probably comprise the most carefully investigated ligand systems, for which the stability and selectivity of metal complex formation has been described successfully in terms of chelate ring size, hole-size-match selectivity, and strain within the ligand backbone.[5] Based on the even higher rigidity and the restriction to exclusively facial coordination, suitable cyclic triamine ligands (see Scheme 1) form a set of

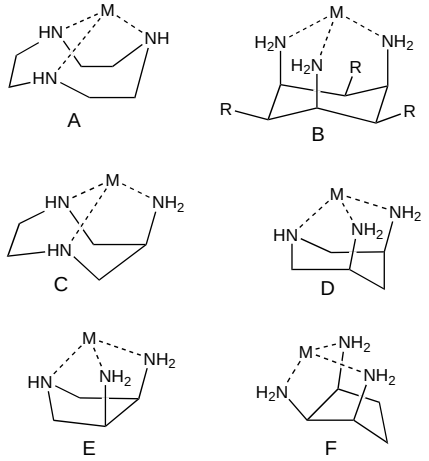

Scheme 1.

ligands for which the individual steric properties can be described in terms of a limited number of parameters: i) the nature of the donating nitrogen atom, which can be attached to the carbon chain as an exocyclic (primary) amino group or can be a part of the ring structure in the form of an endocyclic (secondary) amino group, ii) the size of the different chelate rings (five- or six-membered), and iii) the structure of the ligand backbone, which provides a variable degree of preorientation of the donor groups. 1,4,7-Triazacyclononane (tacn, A),[6] with three endocyclic amino groups, and all-*cis*-cyclohexane-1,3,5-triamine (tach, B, R = H),[7–9] which has exclusively exocyclic amino groups, are both well known. Although both ligands are restricted to facial coordination, they behave significantly differently with regard to metal binding. This becomes immediately evident when the stability constants (log β_2) of the CuL_2 complexes are compared (26.2 for tacn but only 15.5 for tach).[10] It would therefore be of interest to know the properties of the intermediate members C–E (Scheme 1) of this series, in which both exocyclic and endocyclic amino groups are present. However, a search of the literature revealed that a systematic investigation of the metal binding properties of these compounds has not been carried out. In fact, some of the representatives shown are either unknown (C, F), or their metal binding properties have not been investigated (E).[11] For *cis*-3,5-diaminopiperidine (dapi, D) only a study of the coordination chemistry with Pd^{II} appeared in the literature.[12] We have initiated a comparative investigation of the coordination chemistry of the ligands C–F. In the first stage, we have developed efficient preparative procedures for dapi and for *cis*-3,4-diaminopyrrolidine (dap, E). Both ligands can now be prepared in multigram quantities in our laboratory. Interestingly, they exhibit completely different coordination behavior. These results will form a series of papers, starting with the coordination chemistry of dapi. The corresponding results of dap (E)[13] will be reported in a subsequent contribution. In addition we will focus on the possibility of using these ligands as building blocks for more extended ligand systems. This is of particular interest for the ligands C–E, where the simultaneous presence of primary and secondary amino groups allows a selective derivatisation of these compounds.

Results

Ligand synthesis: Although complex formation of *cis*-3,5-diaminopiperidine with Pd^{II} was described some twenty years ago by Schwarzenbach and co-workers,[12] the synthesis of the ligand is not reported. The only description appears in the PhD Thesis of Siroky.[14] We established an improved procedure, which allows a straightforward preparation of dapi as the trihydrochloride salt. Following Siroky's protocol, we converted the commercially available 3,5-dibromopyridine to 3,5-diaminopyridine, which then was hydrogenated stereoselectively to *cis*-3,5-diaminopiperidine. In contrast to Siroky's protocol for which an H_2 pressure of 300 bar was used, we performed the hydrogenation at 5 bar without any loss of yield or diminution in the reaction rate. The analytically pure trihydrochloride is most conveniently obtained from a cation exchange resin. An intermediate conversion to the free base as described by Siroky proved to be unnecessary.

N-substituted derivatives of dapi can be prepared by reductive alkylation (Table 1). The reaction with formaldehyde was carried out in excess formic acid (Eschweiler–Clarke), to yield the permethylated *cis*-pentamethyl-3,5-diaminopiperidine (Me_5dapi).[15] Condensation with aromatic

Table 1. Abbreviation and numbering scheme of ligands.[a]

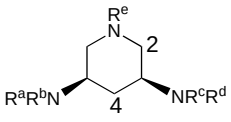

	R^a	R^b	R^c	R^d	R^e
dapi	H	H	H	H	H
Me_5dapi	CH_3	CH_3	CH_3	CH_3	CH_3
bz_2dapi	H	CH_2-C_6H_5	H	CH_2-C_6H_5	H
$(Hhb)_2$dapi	H	*o*-CH_2-C_6H_4-OH	H	*o*-CH_2-C_6H_4-OH	H
pydapi	H	*o*-CH_2-C_5H_4N	H	H	H
py_2dapi	H	*o*-CH_2-C_5H_4N	H	*o*-CH_2-C_5H_4N	H
py_3dapi	H	*o*-CH_2-C_5H_4N	H	*o*-CH_2-C_5H_4N	*o*-CH_2-C_5H_4N

[a] For systematic names: see ref. [15].

  0947-6539/00/0615-2831 $ 17.50+.50/0

aldehydes was carried out in absolute MeOH followed by $NaBH_4$ reduction. With benzaldehyde or salicylaldehyde, doubly substituted derivatives bz_2dapi and $(Hhb)_2$dapi (with the two primary amino groups alkylated) were the sole products,[15] whether the aldehyde was present in a 1:1 molar ratio or in large excess. Neither the mono- nor the trisusbtituted derivative was obtained. This is in contrast to the reaction with the more reactive pyridine-2-carbaldehyde, were the mono-, di-, and trisubstituted derivatives pydapi, py_2dapi, and py_3dapi[15] could be prepared by simple adjustment of the ratio of dapi and the aldehyde.

Protonation and conformation of the free ligands: Acidity constants of H_3dapi^{3+}, $H_3Me_5dapi^{3+}$, and $H_3(Hhb)_2dapi^{3+}$ are listed in Table 2. The permethylated Me_5dapi is considerably

Table 2. pK ($= -\log K$)[a] values of ligands (25 °C, 0.1 mol dm^{-3} KCl).

	H_3dapi^{3+} [b]	$H_3Me_5dapi^{3+}$	$H_3(Hhb)_2dapi^{3+}$
pK_1	4.21	2.6(1)	3.72
pK_2	7.56	6.68	6.74
pK_3	9.47	8.70	8.48
pK_4	–	–	9.88
pK_5	–	–	10.63

[a] $K_i = [LH_{3-i}][H][LH_{4-i}]^{-1}$. The estimated standard deviations are less than 0.01 unless otherwise noted. [b] The values in 0.1 mol dm^{-3} KNO_3 are 4.23, 7.57, and 9.48.

less basic than dapi, which itself is a weaker base than the monobasic piperidine (p$K_a = 11.01$) or cyclohexylamine (p$K_a = 10.62$).[10] A series of pD-dependent ^{1}H NMR measurements were performed in order to establish the protonation sequence of dapi (Figure 1). The assignment of the individual resonances was based on ^{1}H–^{1}H and ^{13}C–^{1}H two-dimensional experiments, and the observed pD dependence of the chemical shifts was modeled with the four macrospecies H_xdapi^{x+} ($3 \geq x \geq 0$) to yield pK_a values of 3.9, 7.5, and 9.4. These pK_a values (D_2O) are in good agreement with those observed in H_2O (Table 2). The H(-C) protons of a polyamine are deshielded by protonation of a nearby basic site. For methylene protons, it has been shown that this effect is linearly related to the fraction of protonation f and that the contributions of different sites are additive. A set of deshielding constants C_{ij} was calculated,[16] for which the deshielding $\Delta\delta_i$ of a methylene proton i by a given basic site j was $\Delta\delta_i^{calcd} = \delta_i^0 + \Sigma_{(j)} C_{ij} f_j$ (δ_i^0 denotes the chemical shift of the non-protonated base). Values for f_j were derived by minimization of $\Sigma(\Delta\delta_i^{obs} - \Delta\delta_i^{calcd})^2$ for the four protons $H2_{ax}$, $H2_{eq}$, $H4_{ax}$, and $H4_{eq}$ (see Figure 1 for the numbering scheme). This procedure gave an excellent agreement between the calculated and observed shifts of the two macrospecies $Hdapi^+$ and H_2dapi^{2+} (Table S3, Supporting Information). The calculations showed that $Hdapi^+$ consists of two micro species with either one of the primary amino groups (79 ± 9%) or the secondary amino group (21 ± 9%) protonated, a ratio which is not too far from a statistical distribution of the proton over the three basic sites. This result is in agreement with the findings for linear polyamines such as diethylenetriamine and triethylenetetramine, for which nearly the same basicities

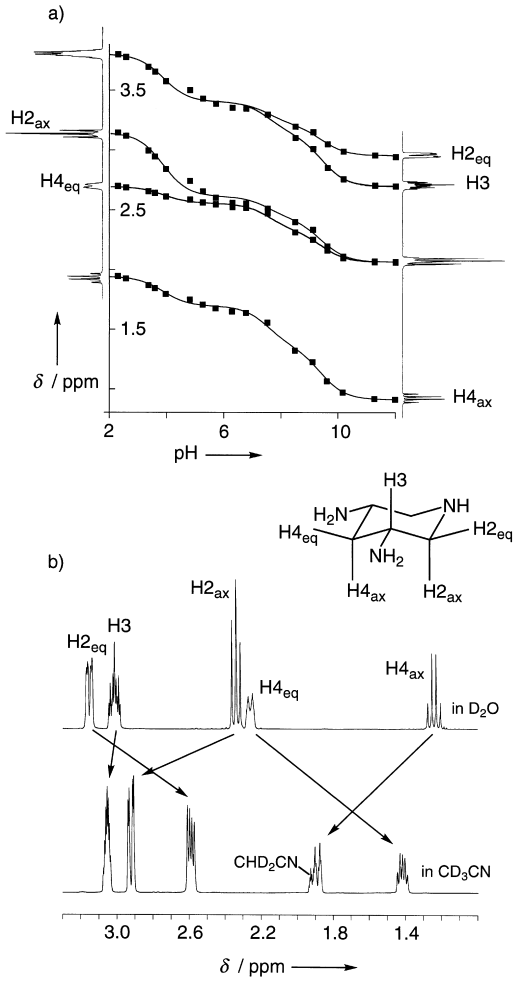

Figure 1. ^{1}H NMR characteristics for H_xdapi^{x+} ($0 \leq x \leq 3$). a) pD dependence of the ^{1}H NMR resonances of dapi in D_2O. Squares correspond to the experimental values, the lines are calculated (minimization of $[\delta_{obs} - \delta_{calc}]^2$), assuming a rapid equilibrium between the species H_xdapi^{x+}. b) ^{1}H NMR spectra of $Hdapi^+$ in D_2O (30 °C) and CD_3CN (60 °C).

have been found for the primary and the secondary amino groups.[16, 17] For H_2dapi^{2+} the species with two protonated primary amino groups predominates slightly (66 ± 9%), as expected for a species with minimal electrostatic repulsion. For H_3dapi^{3+} a chair conformation with equatorial ammonium groups was confirmed by crystal structure analysis (Figure 2). Further evidence for a solution-state chair conformation with the two exocyclic nitrogen donors in equatorial position for all the different protonated forms in D_2O is provided by the ^{1}H–^{1}H coupling constants of the ring H(-C) protons; these remain

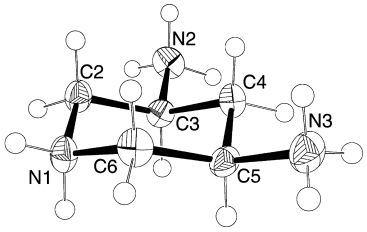

Figure 2. Molecular structure of the protonated H_3dapi^{3+}. The thermal ellipsoids are drawn at the 50% probability level; hydrogen atoms are shown as spheres of arbitrary size. Selected bond lengths [Å]: N1–C2 1.490(3), N1–C6 1.489(3), N2–C3 1.492(3), N3–C5 1.490(3), C2–C3 1.517(3), C3–C4 1.517(3), C4–C5 1.513(3), C5–C6 1.514(3).

0947-6539/00/0615-2832 $ 17.50+.50/0 *Chem. Eur. J.* **2000**, *6*, No. 15

constant throughout the entire pH range investigated. H3 exhibited a sharp triplet of triplets with coupling constants of 12 and 4 Hz (Figure 1). The large value of 12 Hz is characteristic for dihedral angles $H2_{ax}$-C-C-H3 and $H4_{ax}$-C-C-H3 close to 180°. The two equatorial hydrogen atoms $H2_{eq}$ and $H4_{eq}$ exhibited characteristic long-range (w-type) coupling which was not observed for the protons in an axial–axial or axial–equatorial combination. Further support for a chair conformation with equatorial nitrogen donors is provided by the closely related ^{1}H NMR characteristics of dapi and Me_5dapi. For the latter, a structure with axial amino groups can be excluded on the basis of severe repulsion between the bulky dimethylamino groups. There is, however, clear indication that in a non-protic medium such as CH_3CN the monoprotonated $Hdapi^+$ adopts a different conformation, most probably a reversed chair or twisted boat with two axial nitrogen donors, forming an internal N–H···N bridge. The ^{1}H NMR characteristics of the non-protonated dapi in CD_3CN remain the same as in D_2O, whereas for $Hdapi^+$ a dynamic system with broad lines is observed at 30 °C in CD_3CN. At elevated temperatures, the signals become sharp, but the vicinal coupling H2-C-C-H3 and H4-C-C-H3 is significantly reduced, relative to the spectrum in D_2O, and the relative orientation of the chemical shifts is moved in such a way that the formerly axial protons exhibit a characteristic down-field shift (Figure 1b). Similar experiments have been performed for all-*cis*-cyclohexane-1,3,5-triamine (tach). However, for $Htach^+$, the conformation with equatorial nitrogen donors was retained both in D_2O and in CD_3CN. Evidently, the energy required to generate axial amino groups with a chelated proton is much higher for tach than for dapi.

Preparation and structural characterization of metal complexes: $[Co(dapi)_2]^{3+}$ was prepared by aerial oxidation of the Co^{II} precursor in water. ^{1}H NMR spectroscopy shows that the two diastereomers *trans*-$[Co(dapi)_2]^{3+}$ ($\mathbf{1}^{3+}$) and *cis*-$[Co(dapi)_2]^{3+}$ ($\mathbf{2}^{3+}$) are formed in a 1.0:2.8 molar ratio. The observed isomer distribution is in good agreement with the results of molecular mechanics calculations,[18] which revealed almost equal strain energies for the two complexes (the *trans* isomer is favored by 0.5 kJ mol^{-1}). If one accounts for statistical effects (the probability for the formation of $\mathbf{2}^{3+}$ is increased by a factor of two) the calculated ratio $\mathbf{1}^{3+}$:$\mathbf{2}^{3+}$ is 1.0:1.7.

The two isomers could be separated by chromatography. They were characterized by ^{1}H and ^{13}C NMR spectroscopy in solution and crystal structure X-ray analysis in the solid state. The NMR data are in accord with the expected C_{2h} symmetry for $\mathbf{1}^{3+}$ and C_2 for $\mathbf{2}^{3+}$: the ^{13}C NMR spectrum of the chiral complex $\mathbf{2}^{3+}$ exhibited a total of five signals, whereas only three signals were observed for $\mathbf{1}^{3+}$. The crystal structures of both isomers confirmed these assignments (Figure 3).

To enhance their solubility in a non-aqueous medium, $\mathbf{1}Cl_3 \cdot 2H_2O$ and $\mathbf{2}Cl_3$ were converted into the corresponding trifluoromethanesulfonate salts $\mathbf{1}(CF_3SO_3)_3$ and $\mathbf{2}(CF_3SO_3)_3$. In CH_3CN, reaction of these complexes with formaldehyde in the presence of triethylamine yielded crude products, from which the imines $[CoL^a]^{3+}$ ($\mathbf{3}^{3+}$) and $[CoL^b]^{3+}$ ($\mathbf{4}^{3+}$), respectively, could be separated as the major components

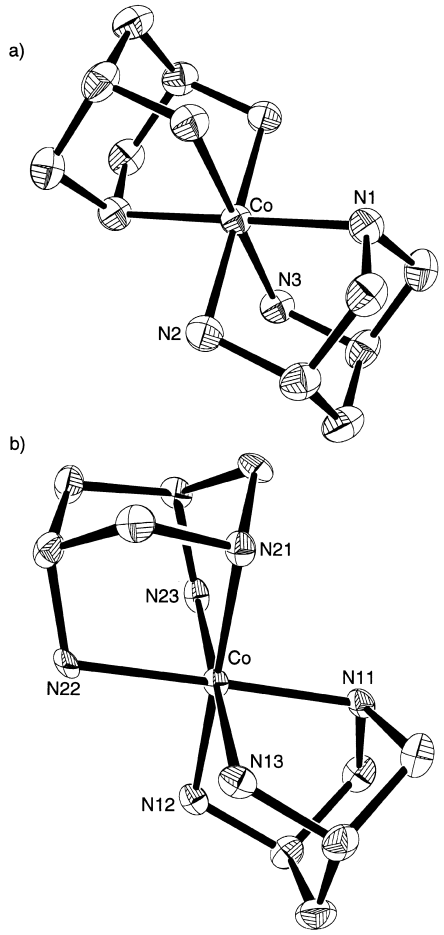

Figure 3. Molecular structure of a) the *trans* isomer $\mathbf{1}^{3+}$ and b) the *cis*-isomer $\mathbf{2}^{3+}$ of $[Co(dapi)_2]^{3+}$. The thermal ellipsoids are drawn at the 50% probability level; hydrogen atoms are omitted. Selected bond lengths [Å] and angles [°] for $\mathbf{1}^{3+}$: Co–N1 1.971(2), Co–N2 1.958(2), Co–N3 1.960(2), N2-Co-N3 86.49(8), N2-Co-N3A 93.51(8), N2-Co-N1 85.88(7), N2-Co-N1A 94.12(7), N3-Co-N1 86.89(7), N3-Co-N1A 93.11(7). Selected bond lengths [Å] and angles [°] for $\mathbf{2}^{3+}$: Co–N21 1.980(3), Co–N22 1.952(3), Co–N23 1.950(3), Co–N11 1.975(3), Co–N12 1.943(3), Co–N13 1.953(3), N12-Co-N23 93.1(1), N12-Co-N22 93.6(1), N23-Co-N22 86.6(1), N12-Co-N13 87.8(2), N23-Co-N13 179.0(1), N22-Co-N13 92.9(1), N12-Co-N11 86.0(1), N23-Co-N11 94.47(1), N22-Co-N11 178.9(1), N13-Co-N11 86.0(2), N21-Co-N12 178.8(1), N23-Co-N21 85.7(1), N22-Co-N21 86.3(1), N13-Co-N21 93.4(1), N11-Co-N21 94.1(1).

(Scheme 2).[15] In both cases the formaldehyde reacted with the coordinated amino groups to yield the corresponding methylideneimines, and additionally some of the imino groups reacted with the intermediate hemiaminals to form species in which the two piperidine rings are fused by N-CH_2-O-CH_2-N bridges.

Crystal structures of the doubly bridged, red *trans*-derivative $\mathbf{3}^{3+}$ and the monobridged, yellow *cis*-derivative $\mathbf{4}^{3+}$ are depicted in Figure 4. It is noteworthy that in $\mathbf{4}^{3+}$ only the four exocyclic nitrogen atoms (i.e., the formerly primary amino groups of the dapi ligands)[19] are involved in either imine formation or as bridgeheads, whereas the two endocyclic nitrogen atoms (i.e., the formerly secondary amino groups) are not affected. In $\mathbf{3}^{3+}$ the two bridges connect an exocyclic nitrogen atom of one piperidine ring with the endocyclic nitrogen atom of the other ring and vice versa, with the two

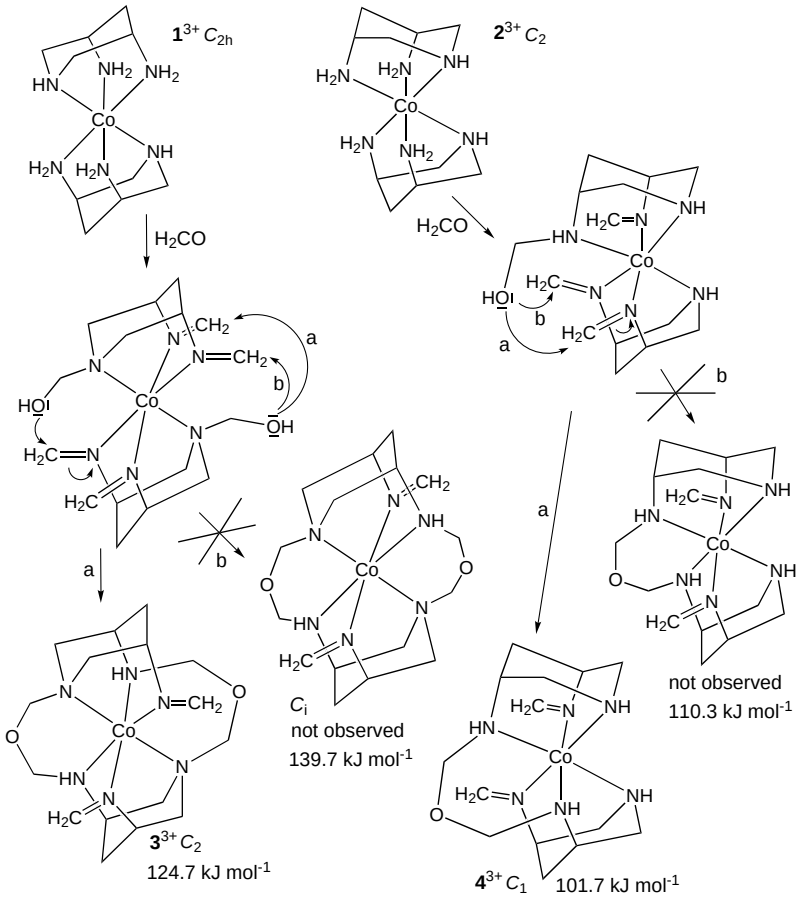

Scheme 2. Proposed mechanistic pathways for the formation of $\mathbf{3}^{3+}$ and $\mathbf{4}^{3+}$ and related isomers together with calculated strain energies [kJ mol^{-1}].

remaining exocyclic nitrogen atoms converted into methylideneimino groups. The sums of the three bond angles around the nitrogen atoms of the methylideneimino groups are 359.8° and 359.9° for $\mathbf{3}^{3+}$, and 359.9° for $\mathbf{4}^{3+}$, which indicates a strictly planar geometry for the sp^2 hybridized donors. In solution, complex $\mathbf{3}^{3+}$ adopts C_2 symmetry with homotopic piperidine rings and consequently, a total of eight signals were observed in the ^{13}C NMR spectrum. They could all be assigned by the usual ^{1}H – ^{13}C and ^{1}H – ^{1}H COSY techniques. Complex $\mathbf{4}^{3+}$ has no symmetry (diastereotopic piperidine rings) and all of the 14 carbon atoms gave individual resonances in the ^{13}C NMR spectrum. Considering the different possibilities for ring closure (Scheme 2) and the configuration at the NH nitrogen atoms of the bridges, a variety of different stereoisomers could form. A series of molecular mechanics calculations showed, however, that the two observed structures $\mathbf{3}^{3+}$ and $\mathbf{4}^{3+}$ clearly represent species of lowest energy. For other isomers, a considerable higher energy (> 8 kJ mol^{-1}) has been calculated, and, in accord with this result, there is no indication that such additional isomers are formed to any significant extent. It should be further noted that even the most favorable of the doubly bridged species ($\mathbf{3}^{3+}$) is substantially strained, as indicated by the observation of some unusually long Co^{III}–N bonds (Table 3). A considerable widening of the coordination sphere is also indicated by the red color of $\mathbf{3}^{3+}$ caused by a characteristic bathochromic shift for the $^1A_{1g} - {}^1T_{1g}$ band ($\lambda_{max} = 491$ nm).[20] For $\mathbf{1}^{3+}$, $\mathbf{2}^{3+}$, and $\mathbf{4}^{3+}$ no unusual Co–N bonds were noted, and the $^1A_{1g} - {}^1T_{1g}$ transition appeared at the lower end of the range expected for a Co^{III} hexaamine complex at 452, 452, and 455 nm, respectively.[21]

The two complexes $[Ni(dapi)_2]^{2+}$ ($\mathbf{5}^{2+}$) and $[Cu(dapi)_2]^{2+}$ ($\mathbf{6}^{2+}$) formed directly in aqueous solution by the combination of hydrated $NiCl_2$ or $Cu(NO_3)_2$ with free dapi in a 1:2 molar ratio. Solid samples of $\mathbf{5}Cl_2 \cdot H_2O$ and $\mathbf{6}(NO_3)_2$ crystallized upon addition of EtOH. Both complexes are labile and the *cis*/*trans* isomers therefore could not be separated. In the solid

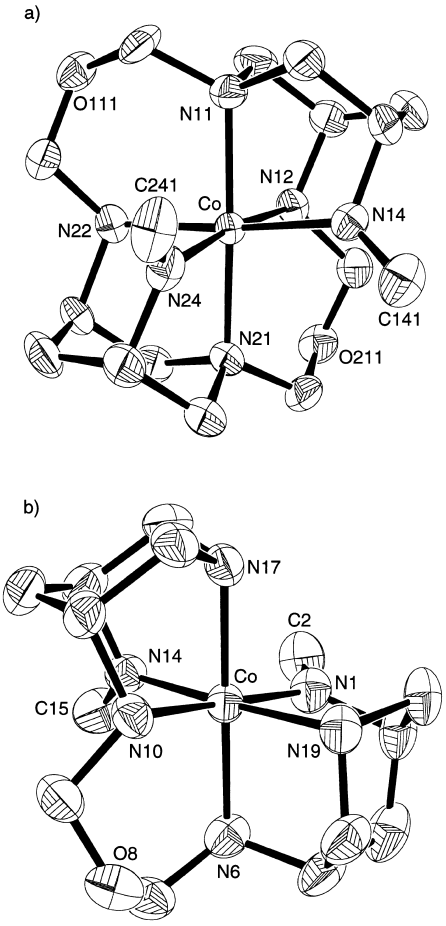

Figure 4. Molecular structure of the two N-CH_2-O-CH_2-N bridged methylideneimino Co^{III} complexes $\mathbf{3}^{3+}$ (a) and $\mathbf{4}^{3+}$ (b). The thermal ellipsoids are drawn at the 50% probability level; hydrogen atoms are omitted. Selected bond lengths [Å] and angles [°] for $\mathbf{3}^{3+}$: Co–N11 2.013(3), Co–N12 1.991(4), Co–N14 1.947(4), Co–N21 2.029(4), Co–N22 1.987(3), Co–N24 1.953(4), N24–C241 1.281(6), N14–C141 1.256(6), N14-Co-N24 91.2(2), N14-Co-N22 173.9(1), N24-Co-N22 86.6(2), N14-Co-N12 86.8(1), N24-Co-N12 173.3(2), N22-Co-N12 96.0(2), N14-Co-N11 84.7(1), N24-Co-N11 101.4(2), N22-Co-N11 90.1(1), N12-Co-N11 84.8(2), N14-Co-N21 100.4(1), N24-Co-N21 84.8(2), N22-Co-N21 85.1(1), N12-Co-N21 89.2(2), N11-Co-N21 171.9(2). Selected bond lengths [Å] and angles [°] for $\mathbf{4}^{3+}$: Co–N1 1.936(4), Co–N6 1.987(4), Co–N10 1.967(4), Co–N14 1.919(4), Co–N17 1.994(4), Co–N19 1.991(4), N1–C2 1.268(7), N14–C15 1.269(7), N14-Co-N1 94.2(2), N14-Co-N10 88.9(2), N1-Co-N10 176.6(2), N14-Co-N6 96.5(2), N1-Co-N6 86.5(2), N10-Co-N6 94.6(2), N14-Co-N19 177.1(2), N1-Co-N19 84.9(2), N10-Co-N19 91.9(2), N6-Co-N19 86.3(2), N14-Co-N17 84.8(2), N1-Co-N17 94.3(2), N10-Co-N17 84.6(2), N6-Co-N17 178.5(2), N19-Co-N17 92.5(2).

0947-6539/00/0615-2834 $ 17.50+.50/0 *Chem. Eur. J.* **2000**, *6*, No. 15

Table 3. Synopsis of structural parameters of the complexes *trans*-$[Co(dapi)_2]^{3+}$ ($\mathbf{1}^{3+}$), *cis*-$[Co(dapi)_2]^{3+}$ ($\mathbf{2}^{3+}$), $[CoL^a]^{3+}$ ($\mathbf{3}^{3+}$),[a] $[CoL^b]^{3+}$ ($\mathbf{4}^{3+}$),[a] *trans*-$[Ni(dapi)_2]^{2+}$ ($\mathbf{5}^{2+}$), *trans*-$[Cu(dapi)_2]^{2+}$ ($\mathbf{6}^{2+}$), $[Cu(dapi)Cl_2]$ (**7**), $[Cd(dapi)Cl_2]_2$ (**8**), $[Co(dapi)(NO_2)(CO_3)]$ (**9**), $[Ni(py_2dapi)Cl]^+$ ($\mathbf{10}^+$), and $[Ni(py_3dapi)]^{2+}$ ($\mathbf{11}^{2+}$).

	$M-N_{endo}$[b] (min, max, mean)	$M-N_{exo}$[b] (min, max, mean)	$M-N(sp^2)$ (min, max, mean)	$M-N_{average}$	Puckering parameters[c]		
					Q	θ	ϕ
$\mathbf{1}^{3+}$		1.958(2)			0.636(3)	167.5(3)	183(1)
		1.960(2)					
	1.971(2)	1.959		1.963			
$\mathbf{2}^{3+}$	1.975(3)	1.943(3)			0.635(4)	166.6(4)	181(2)
	1.980(3)	1.953(3)			0.637(4)	11.9(4)	2(2)
	1.978	1.950		1.959			
$\mathbf{3}^{3+}$	2.013(3)	1.987(3)	1.947(4)		0.646(5)	166.8(4)	174(2)
	2.029(4)	1.991(4)	1.953(4)		0.630(5)	167.8(5)	175(2)
	2.021	1.989	1.950	1.987			
$\mathbf{4}^{3+}$	1.991(4)	1.967(4)	1.919(4)		0.641(5)	14.5(5)	359(2)
	1.994(4)	1.987(4)	1.936(4)		0.626(6)	166.4(5)	179(2)
	1.993	1.977	1.928	1.966			
$\mathbf{5}^{2+}$	2.125(6)	2.113(6)			0.607(9)	10.3(8)	3(5)
	2.141(7)	2.130(7)			0.612(9)	167.2(8)	178(4)
	2.133	2.120		2.124			
$\mathbf{6}^{2+}$		2.040(3)			0.591(5)	171.8(4)	185(3)
		2.059(3)					
	2.409(3)	2.050		2.169			
7	2.363(4)	2.015(2)		2.131	0.587(3)	8.3(3)	0(2)
8		2.331(3)			0.581(4)	11.5(4)	5(2)
		2.369(3)					
	2.401(3)	2.350		2.367			
9	1.995(3)	1.941(2)	1.917(3)	1.949	0.638(3)	11.3(3)	360(2)
$\mathbf{10}^+$		2.059(3)	2.051(3)		0.609(4)	14.7(4)	359(1)
		2.110(3)	2.098(3)				
	2.138(3)	2.085	2.075	2.091			
$\mathbf{11}^{2+}$		2.058(4)	2.076(4)		0.620(5)	14.9(5)	7.6(2)
		2.129(3)	2.100(3)				
	2.117(4)	2.094	2.091	2.096			

[a] For a definition of L^a and L^b see ref. [15]. [b] For the use of the descriptors *exo* and *endo*, see ref. [19]. [c] According to D. Cremer and J. A. Pople (ref. [37]).

samples the *trans* isomers were found exclusively (Figure 5). We attribute this observation to a more favorable packing and lattice energy of the centrosymmetric *trans* isomer rather than to an intrinsically higher stability. As has been shown for Co^{III}, the difference in energy for the two isomers is rather low. In the crystal structures of the *trans* bis-dapi complexes $\mathbf{1}^{3+}$, $\mathbf{5}^{2+}$, and $\mathbf{6}^{2+}$ the metal cations are indeed all placed on crystallographic centers of inversion. The structure of the Ni^{II} complex $\mathbf{5}Cl_2 \cdot H_2O$, which contains two crystallographically independent complex molecules, can be described as an alternating stack of layers parallel to the yz plane at $x = 0$ and $x = 0.5$. In the first layer, the cations are connected by a network of N–H···Cl···H–N and N–H···Cl···H–O(w)···H–N hydrogen bonds. The second layer does not contain water molecules and the cations are connected solely by N–H···Cl···H–N interactions. The Cu^{II} complex $\mathbf{6}^{2+}$ showed a characteristic static Jahn–Teller distortion with four short, equatorial Cu–N bonds (4 exocyclic nitrogen donors, mean Cu–N bond length: 2.05 Å) and two long, axial Cu–N bonds (2 endocyclic nitrogen donors, mean Cu–N bond length: 2.41 Å).[22] The use of $CuCl_2$ and $CdCl_2$ in the above-mentioned preparation procedure resulted in the isolation of the 1:1 complexes $[Cu(dapi)Cl_2]$ (**7**) and $[\{Cd(dapi)Cl_2\}_2]$ (**8**). The former is a mononuclear complex with a distorted square-pyramidal coordinated Cu^{II}, whereas the latter is a dimeric species with a roughly octahedral Cd^{II}, with two terminal and two bridging Cl^- ligands (Figure 6). In both complexes **7** and **8**, the M–N bonds of the endocyclic (secondary) nitrogen donors are considerably longer than the M–N bonds of the exocyclic (primary) nitrogen atoms. A 1:1 complex of Co^{III} was prepared starting from $[Co(NO_2)_6]^{3-}$ and was isolated as

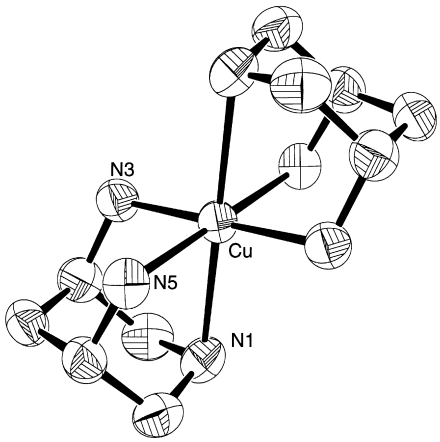

Figure 5. Molecular structure of $[Cu(dapi)_2]^{2+}$ $\mathbf{6}^{2+}$ (the same structure is observed for the Ni^{II} complex $\mathbf{5}^{2+}$). The thermal ellipsoids are drawn at the 50% probability level; hydrogen atoms are omitted. Selected bond lengths [Å] and angles [°] for $\mathbf{6}^{2+}$: Cu–N1 2.409(3), Cu–N3 2.059(3), Cu–N5 2.040(3), N5–Cu-N3A 93.0(1), N5-Cu-N3 87.0(1), N5-Cu-N1A 100.3(1), N5-Cu-N1 79.8(1), N3-Cu-N1 79.2(1), N3-Cu-N1A 100.8(1).

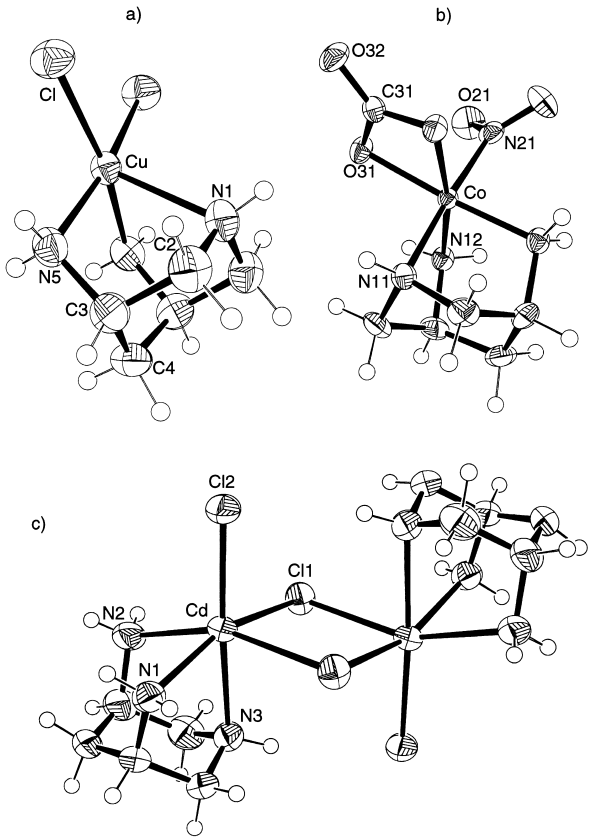

Figure 6. Molecular structure of the 1:1 complexes a) $[Cu(dapi)Cl_2]$ (**7**), b) $[Co(dapi)(NO_2)(CO_3)]$ (**9**), and c) $[(dapi)ClCd\text{-}(\mu_2\text{-}Cl)_2\text{-}CdCl(dapi)]$ (**8**). The thermal ellipsoids are drawn at the 50% probability level; hydrogen atoms are shown as spheres of arbitrary size. Selected bond lengths [Å] and angles [°] for **7**: Cu–N5 2.015(2), Cu–Cl 2.2924(8), Cu–N1 2.363(4), N5-Cu-N5A 88.4(2), N5-Cu-Cl 89.06(8), N5-Cu-Cl(A) 168.89(8), Cl-Cu-Cl(A) 91.42(4), N5-Cu-N1 80.6(1), Cl-Cu-N1 109.65(7). Selected bond lengths [Å] and angles [°] for **8**: Cd–N1 2.331(3), Cd–N2 2.369(3), Cd–N3 2.401(3), Cd–Cl2 2.503(1), Cd–Cl1 2.633(1), Cd–Cl1A 2.713(1), N1-Cd-N2 80.4(1), N1-Cd-N3 75.3(1), N2-Cd-N3 75.2(1), N1-Cd-Cl2 106.34(8), N2-Cd-Cl2 108.03(9), N3-Cd-Cl2 176.50(7), N1-Cd-Cl1 159.41(7), N2-Cd-Cl1 93.72(9), N3-Cd-Cl1 84.09(8), Cl2-Cd-Cl1 94.25(4), N1-Cd-Cl1A 88.07(8), N2-Cd-Cl1A 158.79(8), N3-Cd-Cl1A 84.72(8), Cl2-Cd-Cl1A 92.23(3), Cl1-Cd-Cl1A 90.87(2), Cd-Cl1-Cd 89.14(2). Selected bond lengths [Å] and angles [°] for **9**: Co–N21 1.917(3), Co–O31 1.928(2), Co–N12 1.941(2), Co–N11 1.995(3), O31–C31 1.313(3), O32–C31 1.245(4), N21–O21 1.234(2), C31–O32 1.245(4), C31–O31 1.313(3), N21-Co-O31 91.34(9), O31-Co-O31A 68.2(1), N21-Co-N12 91.18(9), O31-Co-N12 169.74(8), O31-Co-N12 101.81(8), O31-Co-N12 169.74(8), N12-Co-N12A 88.1(1), N21-Co-N11 176.1(1), O31-Co-N11 91.89(9), N12-Co-N11 86.02(9), O32-C31-O31 124.6(1), O21-N21-O21 120.2(3).

$[Co(dapi)(NO_2)(CO_3)]$ (**9**, Figure 6b). Once again, the Co–N bond of the endocyclic nitrogen donor [1.995(3) Å] is considerably longer than the corresponding bonds to the exocyclic nitrogen donors [1.941(2) Å]. The shortest Co–N bond [1.917(3) Å] is observed for the NO_2^- ligand.

For the preparation of the Ni^{II} complexes $[Ni(py_2dapi)Cl]^+$ (**10**$^+$) and $[Ni(py_3dapi)]^{2+}$ (**11**$^{2+}$), the hydrochlorides could be used directly. A preceding deprotonation of the pentadentate $H_5py_2dapi^{5+}$ or the hexadentate $H_6py_3dapi^{6+}$ was not necessary. The two Ni^{II} complexes are evidently of sufficient stability to be formed completely even in an acidic medium. They were isolated in crystalline form as **10**ClO_4 and **11**$(ClO_4)_2 \cdot H_2O$. For both compounds a crystal structure analysis was performed (Figure 7). In the structure of **10**ClO_4, the remaining coordination site is occupied by a Cl^- ligand and the cations are arranged to pairs by two N_{endo}–H···Cl hydrogen bonds [N···Cl distance 3.312(5) Å, H···Cl distance 2.52(4) Å, N–H···Cl angle 177.3(4)°]. Both cations **10**$^+$ and **11**$^{2+}$ have a related completely asymmetric

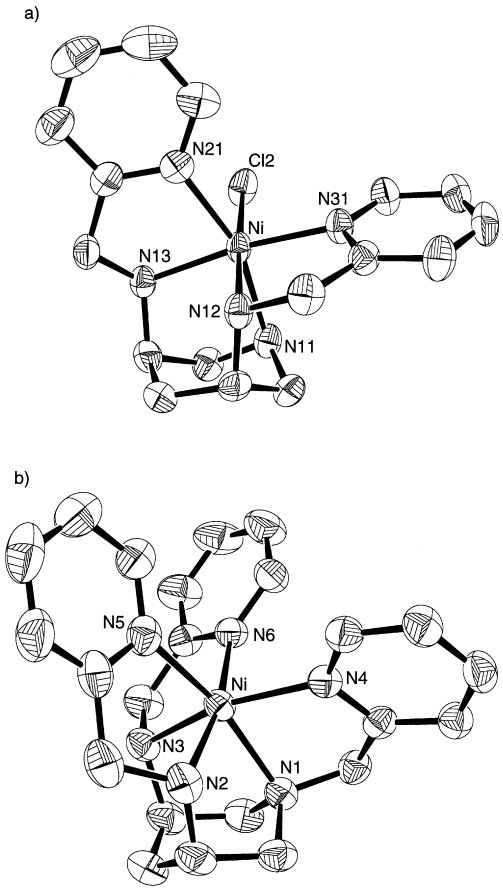

Figure 7. Molecular structure of a) $[Ni(py_2dapi)Cl]^+$ (**10**$^+$) and b) $[Ni(py_3dapi)]^{2+}$ (**11**$^{2+}$). The thermal ellipsoids are drawn at the 50% probability level; hydrogen atoms are omitted. Selected bond lengths [Å] and angles [°] for **10**$^+$: Ni–N11 2.138(3), Ni–N12 2.110(3), Ni–N13 2.059(3), Ni–N21 2.098(3), Ni–N31 2.051(3), Ni–Cl2 2.396(1), N31-Ni-N13 171.4(1), N31-Ni-N21 104.0(1), N13-Ni-N21 80.4(1), N31-Ni-N12 81.5(1), N13-Ni-N12 91.0(1), N21-Ni-N12 92.4(1), N31-Ni-N11 92.8(1), N13-Ni-N11 82.0(1), N21-Ni-N11 161.7(1), N12-Ni-N11 82.9(1), N31-Ni-Cl2 97.20(9), N13-Ni-Cl2 90.10(9), N21-Ni-Cl2 90.14(8), N12-Ni-Cl2 177.40(9), N11-Ni-Cl2 94.95(9). Selected bond lengths [Å] and angles [°] for **11**$^{2+}$: Ni–N1 2.117(4), Ni–N2 2.058(4), Ni–N3 2.129(3), Ni–N4 2.100(3), Ni–N5 2.097(4), Ni–N6 2.076(4), N2-Ni-N6 168.9(1), N2-Ni-N5 80.0(2), N6-Ni-N5 94.1(1), N2-Ni-N4 95.9(1), N6-Ni-N4 94.6(1), N5-Ni-N4 102.3(1), N2-Ni-N1 82.7(1), N6-Ni-N1 103.05(1), N5-Ni-N1 162.7(1), N4-Ni-N1 79.4(1), N2-Ni-N3 90.2(1), N6-Ni-N3 81.0(1), N5-Ni-N3 96.5(1), N4-Ni-N3 160.9(1), N1-Ni-N3 83.6(1).

(chiral) structure with either an *R*,*R* or *S*,*S* configuration of the two exocyclic nitrogen donors. In the hexaamine complex **11**$^{2+}$, the three five-membered chelate rings of the N-CH_2-py pendant arms exhibit a $\Lambda(\delta\delta\lambda)$ configuration with only minor puckering. In the pentaamine complex **10**$^+$ the two N-CH_2-py pendant arms have a $\delta\lambda$ configuration. The coordination octahedron of the Ni^{II} centers is considerably distorted. For **11**$^{2+}$, this distortion can be described as a significant twist

  0947-6539/00/0615-2836 $ 17.50+.50/0 *Chem. Eur. J.* **2000**, *6*, No. 15

towards a trigonal prismatic geometry. The angle which describes the orientation of the two triangles defined by the three sp^3 and the three sp^2 nitrogen donors is 44.3° (octahedron: 60°, trigonal prism: 0°).[23] In both complexes, the *trans* N-Ni-N angles fall in the range of 160.9–171.4° and the *cis*-N-Ni-N angles are in the range 79.4–104.0°. The difference in Ni–N bond lengths for the three types of nitrogen donors is relatively minor. The distances from Ni to the exocyclic and pyridine nitrogens is almost equal, whereas the distance to the endocyclic nitrogen donor is somewhat longer.

Determination of stability constants: The stability of $[M(dapi)]^{2+}$ and $[M(dapi)_2]^{2+}$ has been examined for M = Co^{II}, Ni^{II}, Cu^{II}, Zn^{II}, and Cd^{II} in dilute aqueous solution ($\mu = 0.1$ mol dm^{-3}, 25 °C) by means of pH-metric titrations. The formation of the Ni^{II} complexes proved to be slow and a batch method with individually sealed sample solutions was therefore used.[24] Formation constants are presented in Table 4. For Co^{II}, Ni^{II}, Cu^{II}, and Zn^{II} the measurements were performed in 0.1 mol dm^{-3} KCl. Due to the low stability of the corresponding chloro complexes $[MCl_x]^{2-x}$ a competitive binding of Cl^- is not to be expected.[10] This is in contrast to Cd^{II}, for which a value of 33 mol^{-1} dm^3 has been reported for the formation constant $K^{Cl} = [CdCl^+][Cd^{2+}]^{-1}[Cl^-]^{-1}$. Our experiments in 0.1 mol dm^{-3} KCl and 0.1 mol dm^{-3} KNO_3 did indeed give a significantly lower stability constant for $[Cd(dapi)_2]^{2+}$ in the chloride medium. This effect can be described in terms of conditional formation constants β_n^{cond} (which correspond to the actual experimental quantities) as defined in Equation (1).[25] If we ignore multiple binding of Cl^- to Cd^{2+}, and neglect interactions between $[CdL_n]^{2+}$ and Cl^-, Equation (1) gives rise to Equation (2).

$$\beta_n^{cond} = [Cd'L_n][Cd']^{-1}[L]^{-n} = \{\Sigma_x[CdCl_xL_n]\}\{\Sigma_y[CdCl_y]\}^{-1}[L]^{-n} \quad 0 \le x,y \le 3 \qquad (1)$$

$$\beta_n^{cond} = [CdL_n]\{[Cd] + [CdCl]\}^{-1}[L]^{-n} = [CdL_n][Cd]^{-1}\{1 + K^{Cl}[Cl^-]\}^{-1}[L]^{-n} = \beta_n\{1 + K^{Cl}[Cl^-]\}^{-1} \qquad (2)$$

With $K^{Cl} = 33$ mol^{-1} dm^3 and $[Cl^-] = 0.1$ mol dm^{-3} the expected ratio β_n/β_n^{cond} is 4.3 and consequently the difference in $\log \beta_n$ should be 0.63 for the KNO_3 and KCl medium. This is in excellent agreement with $\log \beta_2$, which is 12.33(2) (KNO_3) and 11.72(2) (KCl). However, for β_1 the observed difference is much smaller. According to Equation (1), this must be interpreted in terms of a significant formation of a mixed species $[Cd(dapi)Cl]^+$. With the values $\beta_1 = 6.87(1)$ (KNO_3) and 6.71(1) (KCl) one can estimate a formation constant of about 20 mol^{-1} dm^3 for the reaction $[Cd(dapi)]^{2+} + Cl^- \rightleftharpoons [Cd(dapi)Cl]^+$. The isolation of the dinuclear [Cl(dapi)Cd-(μ-Cl)$_2$-Cd(dapi)Cl] from a solution with a molar ratio Cd:dapi = 1:2 (Figure 6c) is a further confirmation for the possible interactions of the 1:1 complex $[Cd(dapi)]^{2+}$ with Cl^-. It must, however, be emphasized that the composition of isolated solids does not necessarily represent the species formed in dilute solution. For Cu^{II}, a mixed $[Cu(dapi)Cl_2]$ complex was also observed in the solid phase, even though there was no indication of any Cu–Cl interaction in dilute aqueous solution.

Table 4. Formation constants log K_1 and log K_2 (25 °C, $\mu = 0.1$ mol dm^{-3}) for dapi (L) complexes of divalent metal cations.[a]

M^{II}	log K_1[b]	log K_2[b]
Co	8.44(2)	7.07(3)
Ni	11.33(6)	9.89(6)
Cu	11.42(1)	8.72(2)
Zn	7.93(2)	6.49(3)
Cd[c]	6.87(1)	5.46(2)
Cd[d]	6.71(1)	5.01(2)

[a] $K_1 = [ML][M]^{-1}[L]^{-1}$, $K_2 = [ML_2][ML]^{-1}[L]^{-1}$. [b] The uncertainties given in parentheses correspond to $3 \times \sigma$ calculated by SUPERQUAD.[47] [c] 0.1 mol dm^{-3} KNO_3. [d] 0.1 mol dm^{-3} KCl.

Schwarzenbach presented values for the stability constants of Co^{II}, Ni^{II}, and Cu^{II} complexes of dapi at 20 °C and an ionic strength of 0.1 mol dm^{-3},[12b] referring to "unpublished work" (further information on conditions and methods is not given). Considering the difference in the temperature, the agreement between Schwarzenbach's data and our results for Ni^{II} and Cu^{II} is good. However, for Co^{II}, Schwarzenbach's value for log K_2 is significantly higher. We do not have any explanation for this difference.

Cyclic voltammetry: The redox properties of $[Co(dapi)_2]^{3+}$ ($\mathbf{1}^{3+}$ and $\mathbf{2}^{3+}$) and $[Ni(dapi)_2]^{2+}$ ($\mathbf{5}^{2+}$) were investigated by cyclic voltammetry. For comparison, corresponding complexes with the two triamine ligands taci (1,3,5-triamino-1,3,5-trideoxy-*cis*-inositol) and tmca (all-*cis*-2,4,6-trimethoxycyclohexane-1,3,5-triamine) were also studied (Scheme 1, B; R = OH, OCH_3). The results (Table 5) clearly illustrate quasi-reversible electron transfer for all the $[ML_2]^{2+/3+}$ couples studied (Figure 8). The linear I versus $\sqrt{\nu}$ behavior indicated a diffusion controlled process. For both Ni and Co, the $[ML_2]^{2+/3+}$ potentials of dapi are slightly more negative (less positive) than those of taci and tmca. The less positive values observed for the dapi complexes indicate that oxidation of the $[M(dapi)_2]^{2+}$ species is a slightly more favorable process. In terms of over-all stability constants of two different tridentate

Table 5. Electrochemical data from cyclic voltammetry for $[CoL_2]^{2+/3+}$ and $[NiL_2]^{2+/3+}$ couples in aqueous solution.[a]

$[ML_2]^{2+/3+}$[b]	E° [V][c]	ΔE_p [mV][d]	R [e]
$[Co(dapi)_2]$[f]	−0.43	77, 123	1.0000
$[Co(taci)_2]$	−0.39	77, 145	0.9997
$[Co(tmca)_2]$	−0.36	73, 167	0.9998
$[Ni(dapi)_2]$	0.91	73, 101	0.9991
$[Ni(taci)_2]$	0.97	84, 195	0.9999
$[Ni(tmca)_2]$	0.97	73, 199	0.9999

[a] Some slightly different redox potentials have previously been reported for $[Co(taci)_2]^{2+/3+}$ and $[Co(tmca)_2]^{2+/3+}$ (see refs. [27] and [28]). The difference is due to problems encountered in accurate calibration of the reference electrode. For consistency, the data presented here were all measured under identical conditions at 25 °C giving a relative accuracy better than 0.01 V. [b] dapi = *cis*-3,5-piperidinediamine; taci = 1,3,5-triamino-1,3,5-trideoxy-*cis*-inositol; tmca = all-*cis*-2,4,6-trimethoxy-cyclohexane-1,3,5-triamine. [c] Redox potentials, relative to NHE (Ag/AgCl reference = 207 mV). [d] Peak separation for a scan rate of 5 mV s^{-1} and 1000 mV s^{-1}, respectively. [e] Correlation coefficients for the linearity I versus $\sqrt{\nu}$ in the range 5 mV s^{-1} $\le \nu \le$ 1000 mV s^{-1} with a total of 13 data points for each complex. [f] *cis*-Isomer.

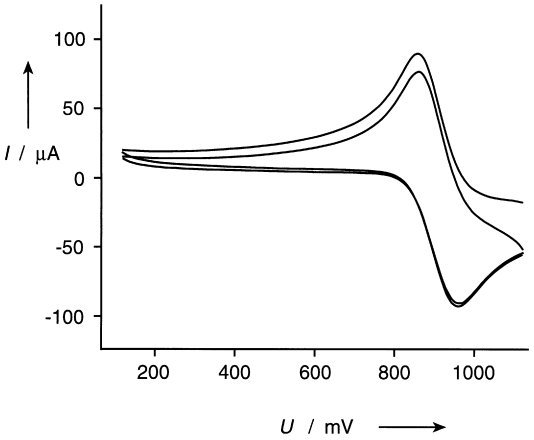

Figure 8. Cyclic voltammogram for $[Ni(dapi)_2]^{2+/3+}$ in aqueous solution (25 °C, U calculated for a NHE reference).

triamine ligands L and L′, Equation (3) (ΔE is the difference in the observed redox potentials for $[ML_2]^{2+/3+}$ and $[ML_2']^{2+/3+}$, $s = 0.059$ V at 25 °C) can be used to estimate the ratio $\beta([ML_2]^{3+})/\beta([ML_2]^{2+})$.

$$\log\{\beta([ML_2]^{3+})/\beta([ML_2]^{2+})\} - \log\{\beta([ML_2']^{3+})/\beta([ML_2']^{2+})\} = \Delta E/s \quad (3)$$

This ratio is increased for dapi relative to taci and tmca by about one order of magnitude. For $[Co(dapi)_2]^{3+}$, both the *cis* and the *trans* isomers gave the same redox potential within experimental error. This is not surprising, because the Co^{II} complex is labile and is expected to undergo rapid isomerisation. Furthermore, even if the two isomers were sufficiently robust to survive the voltammetric cycle, their similar strain energies would be expected to lead to very similar voltammetric properties.[26]

Discussion

Ligand design: The results of our study clearly confirmed the suitability of dapi as a building block for the design of novel, tailored chelators. Firstly, dapi itself exhibited interesting coordination properties and proved to be a rather efficient, facially coordinating ligand for late divalent transition metal cations such as Ni^{II}. Secondly, the dapi unit can readily be extended to ligands of higher denticity. In our study, the reaction with a suitable aldehyde, followed by reduction of the intermediate condensation product proved to be a particularly elegant and simple method. Related procedures have also been successfully used for the alkylation of the cyclic triamine ligands tach,[29] taci[30, 31] (Scheme 1, B; R = H, OH, respectively), and tacn[32] (Scheme 1, A). However, partial alkylation of these C_3-symmetric ligands, with three *equal* amine functions, proved difficult.[31, 33] The ligand dapi is unique in having two different types of amino groups which exhibited different reactivity. With formaldehyde, the peralkylated Me_5dapi was formed. This compound has, however, a low affinity towards metal cations (the conformation with axial amino groups is not accessible) and was only prepared to study the influence of increasing alkylation on conformation and basicity. If a reactive aromatic aldehyde such as pyridine-2-carbaldehyde is used in excess, all three amino groups are monosubstituted and the potentially hexadentate py_3dapi is formed. With less reactive aldehydes, such as salicylaldehyde or benzaldehyde, only the primary amino groups are alkylated. This is also the case if pyridine-2-carbaldehyde and dapi are employed in a 2:1 molar ratio. Hexadentate coordination of py_3dapi and pentadentate coordination of py_2dapi have been confirmed in their Ni^{II} complexes $\mathbf{10}^{+}$ and $\mathbf{11}^{2+}$ (Figure 7). If pyridine-2-carbaldehyde and dapi are employed in a 1:1 molar ratio, it is also possible to prepare the monosubstituted pydapi. Ligands having a denticity less than six are of particular interest, since their metal complexes allow the binding of additional labile ligands as required for catalytic applications.[34]

A somewhat different approach for obtaining extended ligand systems by reductive alkylation is represented in the linking of two ligand molecules by using an inert bis complex $[M(dapi)_2]^{z+}$ as template. This strategy has been developed by Sargeson's group and has recently been applied for taci and tmca.[35] In our present investigation, we have demonstrated that the two isomeric $[Co(dapi)_2]^{3+}$ complexes $\mathbf{1}^{3+}$ and $\mathbf{2}^{3+}$ react readily in a non-aqueous medium to give the two bridged imines $\mathbf{3}^{3+}$ and $\mathbf{4}^{3+}$. In both compounds, two coordinated methylidene-imino groups are formed which have potential to be utilized as electrophiles for subsequent synthetic procedures. In addition, the two dapi frameworks are linked by N-CH_2-O-CH_2-N bridges. These bridges are the result of a ring closure in an intermediate, which has an imino group and a hemi-aminal group in adjacent positions (Scheme 2). Such N-CH_2-O-CH_2-N bridge formation in the reaction of Co^{III} amine complexes with formaldehyde has been previously reported.[36]

The results of our study confirmed that it is possible to connect two dapi units by using a suitable template. Both complexes $\mathbf{3}^{3+}$ and $\mathbf{4}^{3+}$ are completely stable in an acidic aqueous medium. It must, however, be noted that the N-CH_2-O-CH_2-N bridges of the free (demetalated) ligands L^a and L^b would probably be sensitive towards hydrolysis and their isolation is expected to be a difficult task. We regard these two species as interesting models for bridged dapi complexes rather than as precursors for the preparation of the free hexadentate ligands.

Structural properties of dapi complexes

Conformation: The conformation of the six membered piperidine ring can be described by means of the puckering parameters Q, θ, ϕ (Table 3),[37] where the two phase angles θ and ϕ describe the type of conformation. $\theta = 0 \pm n \times 180°$ is indicative of a chair, $\theta = 54.7 \pm n \times 180°$ and $\phi = 0 \pm n \times 60°$ correspond to an envelope conformation. For a twisted boat, the value of ϕ is $0 \pm n \times 60° + 30°$. The puckering parameters of H_3dapi^{3+} [$\theta = 177.7(2)°$] indicate an almost regular chair conformation. This is different from the piperidine rings in the metal complexes, which all exhibit a significant distortion towards an envelope conformation. For the Co^{III}, Ni^{II}, and Cd^{II} complexes, the deviation from $\theta = 0°$ or $\theta = 180°$ is about 11 – 13°. For the two Cu^{II} complexes $\mathbf{6}^{2+}$ and **7**, this distortion is smaller with deviations of 8.2(4)° and 8.3(3)°, respectively.

  0947-6539/00/0615-2838 $ 17.50+.50/0 *Chem. Eur. J.* **2000**, *6*, No. 15

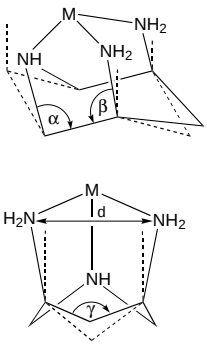

Scheme 3.

The phase angle ϕ is close to 0°, 180°, or 360° for all metal complexes (no distortion towards a twisted boat). Inspection of the appropriate C-C-C and C-C-N angles revealed some characteristic deviation from the ideal value of 109.5°. The C-C-N angles α and β (Scheme 3) fall in the range of 104.6(2)° (mean value for the Co complexes **1**$^{3+}$, **2**$^{3+}$, and **9**) to 108.9(2)° (mean value for the Cd complex **8**). The distortion of the piperidine ring can thus be interpreted in terms of a rearrangement that brings the nitrogen donors closer to the metal center, and this effect decreases with increasing ionic radius. Evidently, the bite angle of the two five-membered chelate rings is too large for the metal centers under investigation. On the other hand the C-C-C angle γ is somewhat enlarged (Co: 112.4(2)°, Cd: 114.5°), and the increase of γ is paralleled by an increase of the intraligand N···N distance *d* between the two exocyclic amino groups (Co: 2.69(1) Å, Cd: 3.03 Å, Scheme 3). This effect increases with increasing ionic size, indicating that the bite angle of the six-membered chelate ring is too small for the metal ions. The observed structure of the dapi complexes thus represent a compromise between the different steric requirements of five- and six-membered chelate rings.[38]

Interligand repulsion in the bis complexes: It is of interest to compare the dapi ligand with triamine ligands that are based on the all-*cis*-1,3,5-cyclohexane-triamine framework, such as tach, taci, or tmca (Scheme 1, B, R = H, OH, OCH_3, respectively). The hydrocarbons which correspond to the structure of a 1:1 complex ML are adamantane for the tach-type ligands and nor-adamantane for dapi. As is well known, adamantane is a low-strain molecule, whereas nor-adamantane is considerably more strained.[39] One would thus expect that the adamantane-type structure of the tach-type ligands would be particularly suited for small cations, whereas dapi would preferentially accommodate cations of much larger size.[40] This is, however, not the case. Molecular mechanics calculations indicated that the optimal M–N bond length in an ML_2 complex is about 1.95 Å for dapi and 1.98 Å for tach. This is a consequence of the interligand repulsion between the two ligand molecules L in a 1:2 complex or between L and the remaining water ligands in a 1:1 complex. The different degree of interligand repulsion in the bis complexes with tach-type or dapi ligands is of particular significance for small metal cations, such as low-spin Co^{III}, and is mainly due to N–H···H–N repulsion. For $[Co(tmca)_2]^{3+}$[27] six short interligand N–H···H–N interactions with a mean H···H distance of 1.956 Å are present,[41] whereas in $[Co(dapi)_2]^{3+}$ only two interligand N–H···H–N distances (*cis*-isomer: 2.25 Å, *trans* isomer: 2.08 Å) are smaller than 2.4 Å (van der Waals radius of H: 1.2 Å).[42] $[Co(tmca)_2]^{3+}$ did indeed exhibit somewhat elongated Co^{III}–N bonds (1.98 Å),[27] while the mean Co–N bond lengths of **1**$^{3+}$ and **2**$^{3+}$ all fall within the normal range of 1.95–1.96 Å (the particularly long Co–N bonds of the macrocyclic derivative **3**$^{3+}$ are evidently caused by the steric demands of the two N-CH_2-O-CH_2-N bridges). These interligand N–H···H–N interactions decrease significantly with increasing ionic size and are no longer operative in a complex with a sufficiently large metal center such as Cd^{II}.

Coordination geometry: The deviation of the MN_6 unit of a *trans*-$[M(dapi)_2]^{z+}$ complex such as **1**$^{3+}$, **5**$^{2+}$, or **6**$^{2+}$ from an ideal octahedron can be described in terms of a combination of a trigonal and a tetragonal distortion.[24] For a trigonal antiprism, which is defined by the two triangular donor sets of the ligands, the trigonal distortion represents a stretching of the antiprism along the threefold axis. The stretching is expressed by significantly larger interligand N-M-N bond angles and interligand N···N distances in comparison to the corresponding intraligand parameters. The tetragonal distortion represents a stretching along the pseudo fourfold axis of the MN_6 octahedron. For a *trans*-$[M(dapi)_2]^{z+}$ complex, this is realized by different M–N bond lengths for the exocyclic and the endocyclic nitrogen donors.[19] A survey of the literature for hexaamine complexes revealed only minimal differences for the M–N bond lengths of primary and secondary amines: Co^{III}: 1.965 Å for primary amines (average of 710 structures), 1.968 Å for secondary amines (average of 216 structures); Ni^{II}: 2.097 Å for primary amines (average of 99 structures), 2.097 Å for secondary amines (average of 124 structures).[43] It is noteworthy that for all dapi complexes investigated in this study the M–N bonds of the exocyclic amino groups are shorter than the bonds of the endocyclic amino groups (Table 3). This is also true for the 1:1 complexes **7**–**9**, for the two Ni complexes **10**$^{+}$ and **11**$^{2+}$ with the alkylated dapi derivatives py_2dapi and py_3dapi, and for the two Co^{III} complexes **3**$^{3+}$ and **4**$^{3+}$ with fused ring systems. If one accepts bond lengths as a criterion for bond energy, it seems that the M–N bond to the endocyclic nitrogen donor of dapi is generally weaker than M–N bonds to the two exocyclic amino groups. The pD-dependent NMR experiments did not, however, reveal a significant difference in the basicity of the two types of donor atoms, and the difference in the N–M bond energy is probably due to the intrinsic strain within the M-dapi fragment as discussed above. In agreement with our observations, Schwarzenbach found square planar structures for $[Pd(Hdapi)_2]^{4+}$, $[Pd(Hdapi)(dapi)]^{3+}$, and $[Pd(dapi)_2]^{2+}$,[12] with a bidentate coordination mode and an exclusive binding of Pd^{II} to the two exocyclic amino groups.

Comparison of dapi and the all-*cis*-1,3,5-triamino-cyclohexane-based taci and tmca again reveal characteristic differences in the coordination behavior of the two types of ligands. Both types showed the above-mentioned trigonal distortion in their bis complexes. However, this distortion is generally more pronounced in the dapi complexes (shorter intraligand and longer interligand N···N distances): $[Co(tmca)_2]^{3+}$, for example, has almost regular octahedral coordination with mean intraligand and interligand N···N distances of 2.78 Å and 2.81 Å, respectively.[27] The corresponding values for **1**$^{3+}$ are 2.69 Å and 2.86 Å. Similarly, the mean intraligand and *cis*-interligand N-Co-N angle of **2**$^{3+}$ is 86.4° and 93.6°, whereas for $[Co(tmca)_2]^{3+}$ the deviation from 90° is only 0.2°–1.3°. For Ni^{II} complexes the trigonal distortion is generally larger. But

again, it is the dapi complex $\mathbf{5}^{2+}$ which exhibits more pronounced distortion than $[Ni(taci)_2]^{2+}$ or $[Ni(tmca)_2]^{2+}$.[24, 44]

Complexes with cyclohexane-based *cis*-1,3,5-triamines have no intrinsic tetragonal distortion, and although a bidentate coordination mode has been postulated for $[Cu(tach)_2]^{2+}$ to explain its unusual thermochemical behavior,[8] this has not been confirmed by an unambiguous structure analysis. On the contrary, reaction of $[Pt^{II}(bipy)Cl_2]$ with tach gave rise to $[Pt^{IV}(bipy)(H_{-2}tach)(OH_2)]^{2+}$, rather than a square planar $[Pt^{II}(bipy\text{-}\kappa^2N,N')(tach\text{-}\kappa^2N,N')]^{2+}$.[9] This result clearly illustrates the difficulties in the bidentate coordination of tach. For taci and tmca, which carry additional substituents in the 2-, 4-, and 6-positions, even further destabilization of such a bidentate coordination mode is to be expected.

For the hexadentate py_3dapi, deviation from octahedral geometry is mainly caused by the significant twist towards trigonal prismatic coordination. The twist ($\varphi = 44.3°$) observed for $\mathbf{11}^{2+}$ is considerably larger than that of the corresponding cyclohexanetriamine-based $[Ni(py_3taci)]^{2+}$ ($\varphi = 52.8°$, py_3taci = 1,3,5-trideoxy-1,3,5-tris((2-pyridinylmethyl)amino)-*cis*-inositol).[45]

Stability of metal complexes

The stability characteristics of bis-complexes $[M(dapi)_2]^{2+}$ are a) generally high stability for the complexes with divalent transition and d^{10} metal cations (Table 6, Figure 9), b) a remarkably high "compatibility" of the two ligand moieties in the bis complexes, c) a reverse Ni/Cu selectivity, and d) a rather high Zn/Cd selectivity.

General stability: The NMR data of uncomplexed dapi in D_2O together with the crystal structure of H_3dapi$[ZnCl_4]Cl$ clearly indicate that the free base and the protonated forms $H_x$dapi^{x+} all adopt a chair conformation with equatorial exocyclic nitrogen donors. However, for metal-complex formation, the exocyclic amino groups must have an axial orientation. The amount of energy required for this conversion is directly correlated to the stability of the complex. Although the NMR experiments do not give a quantitative answer to this question, they clearly show that for dapi this energy is significantly smaller than for tach. For Htach$^+$ a structure with axial amino groups and a chelated proton was not observed at all, whereas for Hdapi$^+$ such a structure was found in CD_3CN (but not in D_2O). For tmca, a structure with axial nitrogen donors is observed to some extent even in D_2O, and in acetonitrile this conformer is formed exclusively.[44] The three ligands tach, dapi, and tmca exhibit an increasing degree of preorientation for the three nitrogen atoms, and the remarkably low formation constants of the tach complexes (Table 6) is clearly a consequence of the particularly high energy required for conversion to the appropriate bonding conformation.[8]

Table 6. Comparison of over-all formation constants log β_2 ($\beta_2 = [ML_2][M]^{-1}[L]^{-2}$) for representative triamine ligands[a] (25 °C, μ = 0.1 mol dm^{-3} unless otherwise noted).

	Ni	Cu	Zn
dapi	21.2	20.1	14.4
taci	20.9	18.8	13.6
tmca	25.9	23.6	18.5
tach	16.5	15.5	
tacn		26.2	
tame	17.3	18.7	10.9
2,2-tri	18.6	20.9	14.2
3,3-tri	12.7		
trap	17.4	19.6	11.4

[a] dapi = *cis*-3,5-piperidinediamine (this work, Table 4); taci = 1,3,5-triamino-1,3,5-trideoxy-*cis*-inositol (ref. [24]); tmca = all-*cis*-2,4,6-trimethoxy-cyclohexane-1,3,5-triamine (ref. [44]); tach = all-*cis*-cyclohexane-1,3,5-triamine (ref. [10]); tacn = 1,4,7-triazacyclononane (μ = 0.5, ref. [10]); tame = 1,1,1-tris(aminomethyl)-ethane (μ = 0.5, ref. [10]); 2,2-tri = 1,4,7-triazaheptane (ref. [10]); 3,3-tri = 1,5,9-triazanonane (ref. [10]); trap = 1,2,3-triaminopropane (ref. [4]).

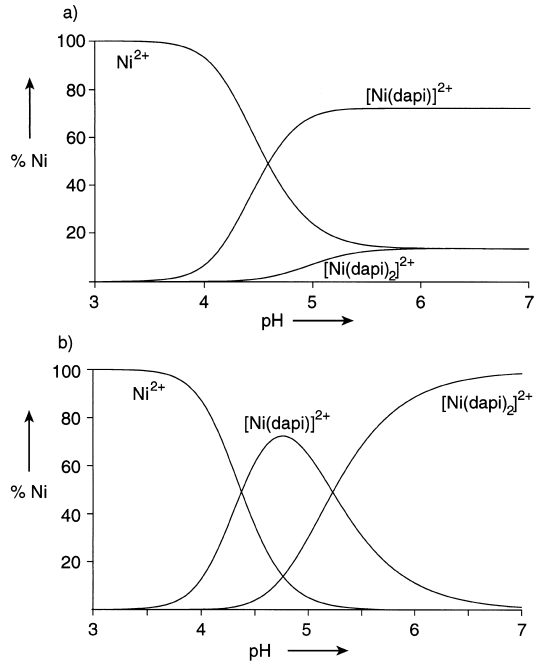

Figure 9. Species distribution plot for an equilibrated aqueous solution of the Ni^{II}-dapi system: a) with equal total concentrations of Ni and dapi (10^{-3} mol dm^{-3}) showing formation of a significant amount of $[Ni(dapi)_2]^{2+}$; b) total Ni 10^{-3} mol dm^{-3}, total dapi = 2×10^{-3} mol dm^{-3}. Only metal containing species are shown. The equilibrium constants listed in Table 4 were used for the calculations.

Compatibility of ligands in bis complexes: The mutual influence of the two tridentate ligands in an octahedral complex can be expressed by the "comproportionation" or "redistribution" reaction [Eq. (4)].

$$M + ML_2 \rightleftharpoons 2\,ML \qquad K_r = [ML]^2[M]^{-1}[ML_2]^{-1} = K_1/K_2 \tag{4}$$

If no mutual influence of the two ligands is assumed (i.e., if ΔH for i) $M + L \rightarrow ML$ and for ii) $ML + L \rightarrow ML_2$ are equal), $K_1 = 16\,K_2$ is expected for statistical reasons,[46] and $\log K_r$ is 1.2. It is noteworthy that for the dapi complexes of Co^{II}, Ni^{II}, Zn^{II}, and Cd^{II}, the experimental values of $\log K_r$ all lie in the narrow range 1.37 – 1.44, and this closely approaches the statistical factor. The larger value for Cu^{II} should probably be interpreted in terms of a change in coordination number. For $[Cu(dapi)_2]^{2+}$ an elongated octahedral coordination has been

0947-6539/00/0615-2840 $ 17.50+.50/0 *Chem. Eur. J.* **2000**, *6*, No. 15

established by the crystal structure determination. There is no reason to doubt that a similar structure is adopted in solution. As a result of its d^9 electron configuration, $[Cu(dapi)]^{2+}$ probably has a coordination number smaller than six. The structure of $[Cu(dapi)Cl_2]$ shown in Figure 6a (with the two Cl^- ligands replaced by H_2O), may serve as a model for such a 1:1 complex in solution.

The low K_r values of the dapi complexes are unique for a saturated triamine (Table 7). If equal amounts of M and L are dissolved in aqueous medium and if complex formation can be considered complete (negligible amount of free L), the ratio $[ML]/[ML_2]$ is $\sqrt{K_r}$ and is independent of the total concentration used. For the Ni^{2+}-dapi system, for example, an aqueous solution of "$[Ni(dapi)]^{2+}$" contains about 16% of the bis complex $[Ni(dapi)_2]^{2+}$ and the same amount of free Ni^{2+} (Figure 9a). This is in marked contrast to tach, for which the proportion of $[Ni(tach)_2]^{2+}$ in an equilibrated 1:1 solution is always less than 1%.

Table 7. Redistribution constant log K_r, ($K_r = [ML]^2[M]^{-1}[ML_2]^{-1} = K_1/K_2$)[a] for selected complexes of divalent metal cations with tridentate amines.

Ligand[a]	Co	Ni	Cu	Zn	Cd
dapi	1.4	1.4	2.7	1.4	1.4
tmca	2.4	3.4	5.3	3.1	2.0
taci	2.5	3.8	5.4	3.2	2.0
tach	2.9	4.1	5.9		
2,2-tri	2.1	2.5	10.9	3.4	2.9
3,3-tri	–	5.6	–	–	–
trap	–	1.8	–	1.6	1.6
tacn	–	–	4.8	–	–

[a] For abbreviations of ligands and references to the formation constants used, see Table 6, footnote [a] and ref. [28] for taci.

Ni^{II}/Cu^{II} and Zn^{II}/Cd^{II} selectivity: The selectivity for these ions is of particular interest since Ni^{II} and Cu^{II} represent cations of similar size but different electronic properties and a correspondingly different coordination geometry, whereas Zn^{II} and Cd^{II} represent cations with the same configuration of the valence electrons but different size. Selectivity for a given pair of cations M and M′ is generally expressed by the metal-exchange reaction given in Equation (5)

$$ML_n + M' \rightleftharpoons M + M'L_n \qquad K_s = [M][M'L_n][M']^{-1}[ML_n]^{-1} = \beta'_n/\beta_n \qquad (5)$$

Ni^{II}/Cu^{II} and Zn^{II}/Cd^{II} selectivity for a variety of tridentate ligands is shown in Table 8. The Zn^{II}/Cd^{II} selectivity of dapi falls in an intermediate range; dapi is more selective for Zn^{II} than the open-chain 1,4,7-triazaheptane (2,2-tri), but less selective than the cyclohexane-based triamines taci and tmca. Similarly, dapi showed intermediate behavior with respect to Ni^{II}/Cu^{II} selectivity. Compared with the flexible open-chain 2,2-tri, the stability of $[Cu(dapi)_2]^{2+}$ is reduced, whereas $[Ni(dapi)_2]^{2+}$ exhibits increased stability. On the other hand, taci and tmca clearly have an even more pronounced selectivity for Ni^{II} (this is not true for tach, however, since $[Cu(tach)_2]^{2+}$ probably does not adopt hexaamine coordination in solution,[8] a direct comparison with this ligand is not possible).

Table 8. Ni^{II}/Cu^{II} and Zn^{II}/Cd^{II} selectivity[a] ($\log K_s$, $K_s = [M][M'L_n][M']^{-1}[ML_n]^{-1} = \beta'_n/\beta_n$) for selected triamine ligands.

	Ni^{II}/Cu^{II} selectivity		Zn^{II}/Cd^{II} selectivity	
	ML	ML_2	ML	ML_2
dapi	– 0.1	1.1	1.1	2.1
taci	0.3	2.2	1.9	2.6
tmca	0.2	2.3	1.9	2.8
2,2-tri	– 5.4	– 2.3	0.5	0.5
2,3-tri[b]	– 5.3	– 1.8	0.8	0.9
3,3-tri	– 5.0	–	1.3	–
trap	–	– 2.2	0.5	1.0

[a] For abbreviations of ligands and references to the formation constants used see Table 6, footnote [a]. [b] 1,4,8-Triazaoctane (ref. [10]).

Structure–stability correlations: Since thermochemical data for the formation of dapi complexes are not available, it is not possible to separate enthalpic from entropic contributions, and a conclusive interpretation of our results is therefore not possible. In particular, the consideration of entropic contributions and of solvation properties is still an unresolved problem.[44] It seems, however, that some of the unique thermodynamic properties of dapi correlate clearly with the structural parameters discussed above.

The low value for the redistribution constant K_r indicates an almost negligible amount of interligand interaction (compared with a hydrated mono complex $[M(dapi)(H_2O)_3]^{2+}$), and the markedly different behavior of dapi and tach-type ligands seems basically to be a consequence of a drastic increase in interligand N–H···H–N repulsion for the latter. This repulsion is particularly high for small cations and consequently dapi showed slightly less positive (more negative) redox potentials for the $[ML_2]^{2+/3+}$ couples than taci or tmca (Table 5). The formation of the oxidized species with the smaller cations in the dapi complexes is favored due to lower interligand repulsion.

The Zn^{II}/Cd^{II} selectivity of dapi is well in line with the analysis given by Hancock, showing that size selectivity is correlated with the type of the chelate rings formed.[38] Zn^{II} and Cd^{II} complexes of ligands that form exclusively five-membered rings, such as 2,2-tri, show almost no selectivity (Table 8). On the other hand, ligands which form exclusively six-membered chelate rings, such as 3,3-tri or the cyclohexane-based taci and tmca, exhibit a preferential binding of Zn^{II}. The dapi ligand forms one six-membered and two five-membered chelate rings and lies, as expected, in-between these two groups.

The reverse order for the Ni^{II}/Cu^{II} selectivity is a general property of rigid, tripodal ligands and is caused by the significant tetragonal (Jahn–Teller) distortion of Cu^{II} hexaamine complexes. In the rigid, facially coordinating dapi the endocyclic nitrogen is forced to form a long and comparably weak Cu–N bond. (This is even true for a 1:1 complex with a non-octahedral geometry, as evident in the crystal structure of $[Cu(dapi)Cl_2]$, Figure 6a.) The contribution of the endocyclic amino group to ΔH is thus relatively minor relative to a flexible ligand such as 2,2-tri, in which a meridional coordination with three short Cu–N bonds can be achieved.[8] On the other hand, the resistance of dapi to tetragonal distortion is smaller than for the C_3-symmetric ligands taci and tmca. In

particular, the bis complexes of these latter ligands with Cu^{II} are destabilized by the enforced tetragonal distortion of the donor set. The structure of dapi does, however, allow a lengthening of the bonds to the endocyclic nitrogen without strain. This nicely explains the observed intermediate behavior of dapi, which has clearly a preference in binding Ni^{II} but is less selective when compared to taci and tmca.

Experimental Section

Safety notes: Formaldehyde and HCl react readily to give the very toxic and volatile bis(chloromethyl)ether. All operations with HCl and formaldehyde must be performed in a fumehood. Solid perchlorate salts of metal complexes with organic ligands are potentially explosive. They should only be prepared in small quantities and must be handled with care.

Physical measurements and analyses: ^{1}H and ^{13}C NMR spectra were measured in D_2O or CD_3CN at 30 °C (unless otherwise noted) on a Bruker DRX 500 MHz NMR spectrometer. Chemical shifts (in ppm) are given relative to sodium (trimethylsilyl)propionate (D_2O) or tetramethylsilane (CD_3CN) as internal standard (= 0 ppm). The pD was adjusted with NaOD and DCl and determined as described previously.[44] C, H and N analyses were performed by H. Feuerhake (Universität des Saarlandes). Mass spectra (FAB^+) were recorded on a Varian MAT 311 instrument (ligands) and on a VG ZAB VSEQ instrument (metal complexes). UV/Vis spectra were measured on a Uvikon 941 spectrophotometer (25 °C) and IR spectra (KBr disks) were recorded on a FT-IR 165 spectrometer (Bio-Rad). Cyclic voltammograms were measured on a BAS C2 cell with a BAS 100B/W 2 potentiostat, with a gold electrode, a platinum counter electrode, and an Ag/AgCl reference electrode at ambient temperature (25 ± 2 °C). The measurements were performed in an aqueous borax buffer (pH 9) with a sample concentration of about 0.002 mol dm^{-3} with KCl (1 mol dm^{-3}) as supporting electrolyte.

Materials: Metal salts which were used for the potentiometric titrations were of highest possible quality (p.a., from Fluka). Pyridine-2-carbaldehyde was a gift of Raschig GmbH (Ludwigshafen). All other chemicals were commercially available products of reagent grade and were used without further purification. Dowex 50WX2 (100 – 200 mesh, H^+ form) and Dowex 2X8 (50 – 100 mesh, Cl^- form) were purchased from Fluka. The OH^- form of the anion resin was obtained from the Cl^- form by elution with 0.3 mol dm^{-3} NaOH, followed by extended rinsing with CO_2-free water until a neutral eluent was observed.

3,5-Diaminopyridine dihydrobromide:[14] 3,5-Dibromopyridine (5 g, 21 mmol), $CuSO_4 \cdot 5H_2O$ (0.17 g, 0.68 mmol), elemental Cu (0.27 g, 4.2 mmol), and 25% aqueous NH_3 (35 mL) were placed in a sealed tube and heated in an oven to 130 °C for 14 h. The clear brownish solution was treated with Mg powder (300 mg) and filtered (removal of Cu). The solution was then evaporated to dryness under reduced pressure and the residue was dried rigorously in vacuo. Aqueous HBr (100 mL, 48%) was added to the resulting solid. The pure 3,5-diaminopyridine dihydrobromide, which precipitated as a pale yellow solid, was separated by filtration and air dried (yield 61%). Elemental analysis calcd (%) for $C_5H_9Br_2N_3$ (271.0): C 22.16, H 3.35, N 15.51, Br 58.98; found C 22.40, H 3.38, N 15.36, Br 58.86; ^{1}H NMR (D_2O): $\delta = 7.58$ (d, $J = 2$ Hz, 2H), 7.14 (t, $J = 2$ Hz, 1H); ^{13}C NMR{^{1}H} (D_2O): $\delta = 149.6$, 121.7, 117.7.

dapi · 3HCl: A solution of 3,5-diaminopyridine dihydrobromide (17.6 g, 65 mmol) and aqueous HBr (12 mL, 48%) in water (200 mL) was placed in a glass autoclave together with 1 g of catalyst (Rh 5% on C) and hydrogenated for 48 h (ambient temperature, 5 bar H_2 pressure). The catalyst was removed by filtration and the resulting clear and colorless solution (pH ≈ 1) was diluted with water to a total volume of 600 mL. The solution was then sorbed on Dowex 50 (H^+ form) and the column was eluted successively with water (600 mL), HCl (600 mL, 0.5 mol dm^{-3}) and finally with HCl (600 mL, 3 mol dm^{-3}). The last fraction was evaporated to dryness at reduced pressure yielding 6.5 g (45%) of a white solid. Elemental analysis calcd (%) for $C_5H_{16}Cl_3N_3$ (224.6): C 26.74, H 7.18, N 18.71, Cl 47.36; found C 26.60, H 7.26, N 18.58, Cl 47.07; ^{1}H NMR (D_2O, pD = 2.3): $\delta = 3.80$ (m, 4H; $H2_{eq}$, H3), 3.15 (t, $J = 12$ Hz, 2H; $H2_{ax}$), 2.70 (m, 1H; $H4_{eq}$), 1.95 (q, $J = 12$ Hz, 1H; $H4_{ax}$); ^{1}H NMR (D_2O, pD = 12.0): $\delta = 2.94$ (dd, $J_1 = 12$ Hz, $J_2 = 3$ Hz, 2H; $H2_{eq}$), 2.70 (tt, $J_1 = 12$ Hz, $J_2 = 3$ Hz, 2H; H3), 2.06 (m, 3H; $H2_{ax}$, $H4_{eq}$), 0.92 (q, $J = 12$ Hz, 1H; $H4_{ax}$); ^{13}C NMR{^{1}H} (D_2O, pD < 2): $\delta = 44.1$ (C2), 43.6 (C3), 31.0 (C4); ^{13}C NMR{^{1}H} (D_2O, pD > 12): $\delta = 54.7$ (C2), 50.0 (C3), 45.1 (C4); MS (FAB^+): *m*/*z* (%): 116.2 (22) $[Hdapi]^+$. Single crystals of composition H_3dapi[$ZnCl_4$]Cl were grown from an aqueous HCl-$ZnCl_2$-EtOH solution.

dapi · 3HNO$_3$: The trihydrochloride was deprotonated by using Dowex 2 (OH^- form) and the resulting solution was acidified with diluted aqueous HNO_3 to pH 1. Addition of EtOH resulted in a quantitative precipitation of dapi · 3HNO_3. Elemental analysis calcd (%) for $C_5H_{16}N_6O_9$ (304.2): C 19.74, H 5.30, N 27.62; found C 20.05, H 5.34, N 27.54.

Me$_5$dapi · 3HCl · 1.75H$_2$O: Solid dapi · 3HCl (500 mg, 2.2 mmol) was dissolved in a mixture of formic acid (80 mL) and water (20 mL). An aqueous solution of formaldehyde (12 mL, 37%) was added, and the solution was refluxed for 12 h. The solution was evaporated to dryness, and the residue was dried rigorously in vacuo and dissolved in aqueous HCl (50 mL, conc). The solution was evaporated to dryness again under reduced pressure, and the resulting white solid (460 mg, 1.4 mmol, 64%) of composition Me_5dapi · 3HCl · 1.75H_2O was dried in air. Elemental analysis calcd (%) for $C_{10}H_{29.5}Cl_3N_3O_{1.75}$ (326.2): C 36.82, H 9.11, N 12.88; found C 37.04, H 8.74, N 12.89; ^{1}H NMR (D_2O, pD < 2): $\delta = 3.94$ (m, 2H; $H2_{eq}$), 3.88 (tt, $J_1 = 12$ Hz, $J_2 = 4$ Hz, 2H; H3), 3.32 (t, $J = 12$ Hz, 2H; $H2_{ax}$), 3.06 (s, 3H; CH_3), 3.02 (s, 12H; CH_3), 2.77 (m, 1H; $H4_{eq}$), 2.15 (q, $J = 12$ Hz, 1H; $H4_{ax}$); ^{1}H NMR (D_2O, pD > 12): $\delta = 3.55$ (tt, $J_1 = 12$ Hz, $J_2 = 4$ Hz, 2H; H3), 3.37 (m, 2H; $H2_{eq}$), 2.96 (s, 12H; CH_3), 2.65 (m, 1H; $H4_{eq}$), 2.53 (s, 3H; CH_3), 2.48 (t, $J = 12$ Hz, 2H; $H2_{ax}$), 1.85 (q, $J = 12$ Hz, 1H; $H4_{ax}$); ^{13}C NMR{^{1}H} (D_2O, pD < 2): $\delta = 60.2$ (C3), 54.0 (C2), 47.5 (CH_3), 43.6 (CH_3), 26.4 (C4); ^{13}C NMR{^{1}H} (D_2O, pD > 12): $\delta = 62.1$ (C3), 55.1 (C2), 47.3 (CH_3), 43.3 (CH_3), 27.3 (C4); MS (FAB^+): *m*/*z* (%): 186.4 (100) $[HMe_5dapi]^+$.

pydapi · 4HCl · 1H$_2$O: dapi · 3HCl (0.5 g, 2.2 mmol) was dissolved in water (10 mL) and passed through a column of Dowex 2 (OH^- form). The alkaline eluent was collected and evaporated to dryness, and the residue was dissolved in absolute MeOH (50 mL). Pyridine-2-carbaldehyde (235 mg, 2.2 mmol) was added and the resulting yellow solution was stirred for 2 h at room temperature. Solid $NaBH_4$ (416 mg, 11 mmol) was added in portions over 1 h. The reaction mixture foamed vigorously. The mixture was adjusted to a pH of about 1 by careful addition of diluted aqueous HCl in a fume hood and sorbed on Dowex 50 (H^+ form). The column was successively eluted with H_2O (500 mL), HCl (500 mL, 0.5 mol dm^{-3}), and HCl (500 mL, 6 mol dm^{-3}). The last fraction was evaporated to dryness in vacuo. The resulting white solid (512 mg, 63%) was air-dried. Elemental analysis calcd (%) for $C_{11}H_{24}Cl_4N_4O$ (370.2): C 35.69, H 6.54, N 15.14; found C 35.64, H 6.49, N 14.48; ^{1}H NMR (D_2O, 1 mol dm^{-3} DCl): $\delta = 8.84$ (m, 1H), 8.60 (m, 1H), 8.14 (m, 1H), 8.05 (m, 1H) (aromatic ring protons), 4.71 (m, 2H; CH_2-N), 3.95 (m, 1H; $H2_{eq}$ or $H6_{eq}$), 3.84 (m, 3H; superposition of $H6_{eq}$ or $H2_{eq}$, H3, $H5_{ax}$), 3.24 (m, 2H; $H2_{ax}$, $H6_{ax}$), 2.86 (m, 1H; $H4_{eq}$), 2.01 (q, $J = 12$ Hz, 1H; $H4_{ax}$); ^{13}C NMR{^{1}H} (D_2O, 1 mol dm^{-3} DCl): $\delta = 149.6$, 146.1, 146.0, 130.1 (aromatic ring carbon atoms), 53.6, 53.3 (C3, C5), 49.0 (CH_2-N), 46.8, 46.4 (C2, C6), 33.3 (C4); according to a ^{1}H – ^{13}C COSY experiment, the signal at $\delta = 130.1$ corresponds to two carbon atoms; MS (FAB^+): *m*/*z* (%): 207.3 (11) $[Hpydapi]^+$.

py$_2$dapi · 5HCl · 3.5H$_2$O: The same procedure as described above for pydapi was used. However, the triamine (4.4 mmol) and pyridine-2-carbaldehyde (8.8 mmol) were employed in a 1:2 molar ratio. The intermediate Schiff base was reduced with $NaBH_4$ (1.66 g, 44 mmol). Workup yielded a white solid (945 mg, 40%). Elemental analysis calcd (%) for $C_{17}H_{35}Cl_5N_5O_{3.5}$ (542.8): C 37.62, H 6.50, N 12.90; found C 37.53, H 6.35, N 12.84; ^{1}H NMR (D_2O, 1 mol dm^{-3} DCl): $\delta = 8.78$ (d, $J = 7$ Hz, 2H), 8.50 (t, $J = 8$ Hz, 2H), 8.02 (d, $J = 8$ Hz, 2H), 7.95 (t, $J = 7$ Hz, 2H) (aromatic ring protons), 4.65, 4.60 (AB system, $J = 15$ Hz, 4H; CH_2-N), 3.88 (dd, $J_1 = 12$ Hz, $J_2 = 4$ Hz, 2H; $H2_{eq}$), 3.68 (tt, $J_1 = 12$ Hz, $J_2 = 4$ Hz, 2H; H3), 3.17 (t, $J = 12$ Hz, 2H; $H2_{ax}$), 2.91 (m, 1H; $H4_{eq}$), 1.90 (q, $J = 12$ Hz, 1H; $H4_{ax}$); ^{13}C NMR{^{1}H} (D_2O, 1 mol dm^{-3} DCl): $\delta = 152.4$, 148.6, 146.5, 129.5, 129.4 (aromatic ring carbon atoms), 53.6 (C3), 49.5 (CH_2-N), 47.5 (C2), 34.0 (C4); MS (FAB^+): *m*/*z* (%): 298.4 (100) $[Hpy_2dapi]^+$.

py$_3$dapi · 6HCl · 2H$_2$O: The same procedure as described above for py$_2$dapi was used. However, a slight excess of pyridine-2-carbaldehyde (1.5 g, 14 mmol) was used. The intermediate Schiff base was reduced with $NaBH_4$ (2.65 g, 70.0 mmol). Workup yielded a white solid (1.32 g, 47%). Elemental

0947-6539/00/0615-2842 $ 17.50+.50/0 *Chem. Eur. J.* **2000**, *6*, No. 15

analysis calcd (%) for $C_{23}H_{38}Cl_6N_6O_2$ (643.3): C 42.94, H 5.95, N 13.06; found C 43.18, H 5.69; N 13.19; ^{1}H NMR (D_2O, 1 mol dm^{-3} DCl): $\delta = 8.93$ (d, $J = 6$ Hz, 2H), 8.80 (d, $J = 6$ Hz, 1H), 8.73 (t, $J = 8$ Hz, 2H), 8.62 (t, $J = 8$ Hz, 1H), 8.30 (d, $J = 8$ Hz, 2H), 8.18 (t, $J = 6$ Hz, 2H), 8.10 (d, $J = 8$ Hz, 1H), 8.04 (t, $J = 6$ Hz, 1H) (aromatic ring protons), 4.84, 4.93 (AB-system, $J = 14$ Hz, 4H; CH_2-N_{exo}), 4.35 (s, 2H; CH_2-N_{endo}), 4.02 (m, 2H; H3), 3.50 (m, 2H; $H2_{eq}$), 3.08 (m, 1H; $H4_{eq}$), 2.80 (t, $J = 11$ Hz, 2H; $H2_{ax}$), 1.98 (q, $J = 12$ Hz, 1H; $H4_{ax}$); ^{13}C NMR{^{1}H} (D_2O, 1 mol dm^{-3} DCl): $\delta = 154.8$, 150.8, 150.3, 147.1, 146.1, 144.2, 131.4, 131.0, 129.8, 129.2 (aromatic ring carbon atoms), 59.7 (CH_2-N_{endo}), 56.3 (C3), 55.5 (C2), 48.1 (CH_2-N_{exo}), 32.0 (C4); MS (FAB$^+$): *m*/*z* (%): 389.2 (100) $[Hpy_3dapi]^+$.

$(Hhb)_2$dapi · 3HCl · 2H_2O: The same procedure as described above for pydapi was used. However, the triamine (2.3 mmol) and salicylaldehyde (4.6 mmol) were employed in exactly a 1:2 molar ratio. The intermediate Schiff base was reduced with $NaBH_4$ (0.85 g, 22 mmol). Recrystallization from concentrated hydrochloric acid yielded a white solid (0.58 g, 53%). Elemental analysis calcd (%) for $C_{19}H_{32}Cl_3N_3O_4$ (472.8): C 48.26, H 6.82, N 8.89; found C 48.26, H 6.86, N 8.77; ^{1}H NMR (D_2O, 1 mol dm^{-3} DCl): $\delta =$ 7.41 (m, 4H), 7.03 (m, 4H), (aromatic ring protons), 4.42, 4.38 (AB system, $J = 13$ Hz, 4H; CH_2-N), 3.95 (dd, $J_1 = 12$ Hz, $J_2 = 4$ Hz, 2H; $H2_{eq}$), 3.81 (tt, $J_1 = 12$ Hz, $J_2 = 4$ Hz, 2H; H3), 3.27 (t, $J = 13$ Hz, 2H; $H2_{ax}$), 3.00 (m, 1H; $H4_{eq}$), 2.10 (q, $J = 12$ Hz, 1H; $H4_{ax}$); ^{13}C NMR{^{1}H} (D_2O, 1 mol dm^{-3} DCl): $\delta = 158.1$, 134.9, 134.7, 123.7, 119.5, 118.6 (aromatic ring carbon atoms), 52.4 (C3), 48.2 (CH_2-N), 46.1 (C2), 31.1 (C4); MS (FAB$^+$): m/z (%): 328.3 (30) $[H(Hhb)_2dapi]^+$.

bz_2dapi · 3HCl · 0.66H_2O: The same procedure as described above for pydapi with 2.3 mmol of the triamine and 9.2 mmol of benzaldehyde was used. The intermediate Schiff base was reduced with $NaBH_4$ (1.3 g, 34 mmol). In contrast to the above described procedure, the solution of the intermediate Schiff base was colorless. Recrystallization from water yielded a white solid (0.50 g, 52%). Elemental analysis calcd (%) for $C_{19}H_{29.33}Cl_3N_3O_{0.66}$ (416.8): C 54.75, H 7.09, N 10.08; found C 54.62, H 7.04, N 9.50; ^{1}H NMR (D_2O, 1 mol dm^{-3} DCl): $\delta = 7.53$ (s, 10H; aromatic ring protons) 4.43, 4.39 (AB-system, $J = 13$ Hz, 4H; CH_2-N), 3.96 (dd $J_1 =$ 12 Hz, $J_2 = 4$ Hz, 2H; $H2_{eq}$), 3.87 (tt, $J_1 = 12$ Hz, $J_2 = 4$ Hz, 2H; H3), 3.26 (t, $J = 12$ Hz, 2H; $H2_{ax}$), 2.98 (m, 1H; $H4_{eq}$), 2.08 (q, $J = 12$ Hz, 1H; $H4_{ax}$); ^{13}C NMR{^{1}H} (D_2O, 1 mol dm^{-3} DCl): $\delta = 132.8$, 132.6 (superposition of two resonances), 132.3 (aromatic ring carbon atoms), 52.3(C3, C5), 52.1 (CH_2-N), 45.8 (C2, C6), 31.0 (C4).

$[Co(dapi)_2]Cl_3$ (1^{3+}, 2^{3+}): dapi · 3HCl (2.5 g, 11 mmol) was dissolved in water (50 mL), and the pH of the solution was adjusted to 8.5 by the addition of NaOH (23 mL, 1 mol dm^{-3}). $CoCl_2 \cdot 6H_2O$ (1.3 g, 5.5 mmol) and charcoal (1 g), suspended in water (100 mL) was then added. A stream of air was passed through the mixture for 12 h, while the temperature was kept at 60 °C. The charcoal was removed by filtration and the yellow solution (pH 7) was acidified with HCl to a pH of 3 and sorbed on Dowex 50. The column was washed successively with water (500 mL), HCl (500 mL, 0.5 mol dm^{-3}, removal of Co^{II}), and the product was then eluted as a yellow fraction with HCl (500 mL, 3 mol dm^{-3}). Evaporation to dryness yielded a yellow solid (1.3 g, 59%). The crude product (1 g) was dissolved in a small amount of water and sorbed on SP-Sephadex C-25. The column was eluted with trisodium citrate (0.2 mol dm^{-3}). Beside several minor bands two major yellow bands (first fraction: *trans*-isomer $\mathbf{1}^{3+}$, second fraction: *cis*-isomer $\mathbf{2}^{3+}$) were collected separately. They were desalted on Dowex 50 (3 mol dm^{-3} HCl) and evaporated to dryness.

Compound ***1*** $Cl_3 \cdot 2H_2O$: Yield: 107 mg (10%); elemental analysis calcd (%) for $C_{10}H_{30}Cl_3CoN_6O_2$ (431.7): C 27.82, H 7.00, N 19.47; found C 27.72, H 6.61, N 19.44; UV/Vis (H_2O): λ_{max} (ε) = 325 (81), 452 nm (64 mol^{-1} dm^3 cm^{-1}); ^{1}H NMR (D_2O, pD = 1): $\delta = 6.22$ (br, 2H; H-N_{endo}), 5.45 (br, 4H; H-N_{exo}), 4.64 (br, 4H; H-N_{exo}), 3.53(m, 4H; H3), 3.00 (m, 8H; $H2_{eq}$, $H2_{ax}$), 2.02 (m, 2H, $H4_{eq}$), 1.89 (m, 2H, $H4_{ax}$); ^{1}H NMR (D_2O, pD = 8): the signals at 6.22, 5.45, and 4.64 (NH protons) disappeared; ^{13}C NMR{^{1}H} (D_2O): $\delta = 59.1$, 52.4, 32.8.

Compound ***2*** Cl_3: Yield: 397 mg (40%); elemental analysis calcd (%) for $C_{10}H_{26}Cl_3CoN_6$ (395.7): C 30.36, H 6.62, N 21.24; found C 30.33, H 6.58, N 20.86; UV/Vis (H_2O): λ_{max} (ε) = 325 (174), 452 nm (110 mol^{-1} dm^3 cm^{-1}); ^{1}H NMR (D_2O, pD = 1): $\delta = 5.86$ (br, 2H; NH), 5.63 (br, 2H; NH), 5.35 (br, 2H; NH); 5.10 (br, 2H; NH), 4.21 (br, 2H; NH), 3.44 (m, 4H; H3, H5), 3.19 (d, $J = 12$ Hz, 2H; $H2_{eq}$ or $H6_{eq}$), 3.12 (d, $J = 12$ Hz, 2H; $H2_{eq}$ or $H6_{eq}$), 2.90 (t, $J = 12$ Hz, 4H; $H2_{ax}$, $H6_{ax}$), 1.97 (m, 4H; $H4_{eq}$, $H4_{ax}$); ^{1}H NMR (D_2O, pD = 8): $\delta = 3.44$ (m, 2H; H3 or H5), 3.42 (m, 2H; H5 or H3), 3.12 (dd, $J_1 =$ 13 Hz, $J_2 = 3$ Hz, 2H; $H2_{eq}$ or $H6_{eq}$), 3.08 (dd, $J_1 = 13$ Hz, $J_2 = 3$ Hz, 2H; $H6_{eq}$ or $H2_{eq}$), 2.92 (m, 4H; $H2_{ax}$, $H6_{ax}$), 2.01 (td $J_1 = 16$ Hz, $J_2 = 3$ Hz, 2H; $H4_{eq}$), 1.91 (td, $J_1 = 16$ Hz, $J_2 = 2$ Hz, 2H; $H4_{ax}$); ^{13}C NMR{^{1}H} (D_2O): $\delta =$ 59.3 (C2 or C6), 58.5 (C6 or C2), 52.1, (C3 or C5) 52.0 (C5 or C3), 32.3 (C4). Single Crystals of composition $\mathbf{1}Cl_3 \cdot 2H_2O$ and $\mathbf{2}Cl_3 \cdot H_2O$ were grown from H_2O/EtOH at 4 °C.

Compound 1$(CF_3SO_3)_3 \cdot 2H_2O$: Compound $\mathbf{1}Cl_3 \cdot 2H_2O$ (0.25 g, 0.58 mmol) was dissolved in triflic acid under N_2, and a stream of dry N_2 was passed through this solution for 3 h at a temperature of about 70 °C. The solution was allowed to cool to room temperature and was poured into diethyl ether (500 mL). A pale yellow precipitate was obtained which was filtered and washed carefully several times with diethyl ether. Yield 400 mg (89%) of the air dried product. Elemental analysis calcd (%) for $C_{13}H_{30}CoF_9N_6O_{11}S_3$ (772.5): C 20.21, H 3.91, N 10.88; found C 20.14, H 3.67, N 10.67.

Compound 2$(CF_3SO_3)_3$: This compound was prepared by the same procedure as described for the *trans*-isomer. Yield: 96% of a pale yellow solid. Elemental analysis calcd (%) for $C_{13}H_{26}CoF_9N_6O_9S_3$ (736.5): C 21.20, H 3.56, N 11.41; found C 21.57, H 3.50, N 10.94.

$[CoL^a]^{3+}$ (3^{3+}):[15] Paraformaldehyde (1.4 g, 47 mmol) and NEt_3 (2.4 g, 24 mmol) were added to a solution of $\mathbf{1}(CF_3SO_3)_3 \cdot 2H_2O$ (0.3 g, 0.38 mmol) in acetonitrile (60 mL). The mixture was stirred at ambient temperature for 30 min. A color change to brown and finally to orange was noted. The reaction was quenched by the addition of H_2SO_4 (18 g in 200 mL of H_2O), and excess paraformaldehyde was carefully removed by filtration. The solution was diluted to 400 mL and sorbed onto Dowex 50. The column was washed with H_2O (500 mL) and HCl (0.5 mol dm^{-3}, 500 mL). The product was eluted (red fraction) with HCl (1.5 mol dm^{-3}, 500 mL), and evaporated to dryness. The solid was redissolved in water and sorbed on SP-Sephadex C-25. Elution with aqueous Na_2SO_4 (0.2 mol dm^{-3} acidified with H_2SO_4 to a pH of 4) yielded several minor fractions and one major red fraction. This major fraction was collected, desalted on Dowex 50, and evaporated to dryness. Yield: 100 mg (47%) of a red solid of composition $\mathbf{3}Cl_3 \cdot 3H_2O$. Elemental analysis calcd (%) for $C_{16}H_{36}Cl_3CoN_6O_5$ (557.8): C 34.45, H 6.51, N 15.07; found: C 34.60, H 6.13, N 15.20; UV/Vis (H_2O): λ_{max} (ε) = 343 (291), 491 nm (160 mol^{-1} dm^3 cm^{-1}); IR (KBr): $\tilde{\nu} = 1643$ cm^{-1} (C=N); ^{1}H NMR (D_2O): $\delta = 8.18$ (d, $J = 7$ Hz, 2H), 7.85 (d, $J = 7$ Hz, 2H), 4.58 (d, $J = 11$ Hz, 2H), 4.56 (m, 2H), 4.45, 4.40 (AB-system, $J = 11$ Hz, 4H), 4.20 (d, $J = 11$ Hz, 2H), 3.90 (d, $J = 11$ Hz, 2H), 3.69 (m, 2H,), 3.35 (d, $J =$ 13 Hz, 2H), 3.04 (d, $J = 13$ Hz, 2H), 2.91 (d, $J = 13$ Hz, 2H), 2.34 (m, 2H), 2.23 (m, 2H); ^{13}C NMR{^{1}H} (D_2O): $\delta = 176.2$, 86.1, 80.6, 70.0, 61.1, 58.7, 53.2, 27.8; MS (FAB$^+$): *m*/*z* (%): 289.1 (34) $[Co(dapi)_2]^+$, 432.2 (27) $[CoL^aCl]^+$. Single crystals of composition $\mathbf{3}[ZnCl_4]Cl$, suitable for X-ray diffraction, were grown from a solution of $\mathbf{3}Cl_3 \cdot 3H_2O$ (30 mg, dissolved in a minimum amount of H_2O), $ZnCl_2$ (24 mg, added in solid form) and aqueous HCl (5 mL, 3 mol dm^{-3}) at room temperature. Elemental analysis calcd (%) for $C_{16}H_{30}Cl_5CoN_6O_2Zn$ (640.0): C 30.03, H 4.72, N 13.13; found C 29.73, H 5.33, N 12.95.

$[CoL^b]^{3+}$ (4^{3+}):[15] This complex was prepared following the protocol reported for $\mathbf{3}^{3+}$, by using $\mathbf{2}(CF_3SO_3)_3$ (1.0 g, 1.4 mmol), paraformaldehyde (4.7 g, 0.16 mol) and NEt_3 (8.1 g, 80 mmol). The resulting yellow solid was dried in vacuo over KOH. Yield: 350 mg (50%) of $\mathbf{4}Cl_3 \cdot 2H_2O$. Elemental analysis calcd (%) for $C_{14}H_{32}Cl_3CoN_6O_3$ (497.7): C 33.78, H 6.48, N 16.88; found C 33.82, H 5.94, N 16.44; UV/Vis (H_2O): λ_{max} (ε) = 323 (125), 455 nm (57 mol^{-1} dm^3 cm^{-1}); IR (KBr): $\tilde{\nu} = 1651$ cm^{-1} (C=N); ^{1}H NMR (D_2O): $\delta =$ 8.27(d, $J = 7$ Hz, 1H), 8.10 (d, $J = 7$ Hz, 1H), 7.98 (d, $J = 7$ Hz, 1H), 7.69 (d, $J = 7$ Hz, 1H), 4.65 (m, 2H), 4.52 (m, 3H), 4.22 (d, $J = 10$ Hz, 1H), 3.84 (d, $J = 13$ Hz, 1H), 3.71 (m, 1H), 3.57 (m, 1H), 3.36 (d, $J = 13$ Hz, 1H), 3.27 (d, $J = 13$ Hz, 1H), 3.10 (m, 4H), 2.91 (d, $J = 13$ Hz, 1H), 2.25 (m, 4H); ^{13}C NMR{^{1}H} (D_2O): $\delta = 178.8$, 175.9, 87.3, 83.1, 73.5, 73.1, 64.7, 60.4, 59.2, 58.9, 56.8 (two C-atoms), 36.5, 31.0. Recrystallization of this product from a $ZnCl_2$/HCl solution yielded single crystals of $\mathbf{4}[ZnCl_4]Cl$.

$[Ni(dapi)_2]Cl_2 \cdot H_2O$ ($5Cl_2 \cdot H_2O$): The ligand dapi · 3HCl (213 mg, 0.9 mmol) was dissolved in water (30 mL) and was deprotonated by using Dowex 2 (OH^- form). $NiCl_2 \cdot 6H_2O$ (113 mg, 0.48 mmol) was added to this solution. The resulting pink solution was evaporated to dryness. Single crystals were grown by redissolution in a minimum amount of water and layering with EtOH. The resulting air dried, pink crystals (133 mg, 0.35 mmol, 78%) were suitable for single crystal X-ray diffraction analysis.

Elemental analysis calcd (%) for $C_{10}H_{28}Cl_2N_6NiO$ (378.0): C 31.78, H 7.47, N 22.23; found C 31.77, H 7.20, N 22.09; MS (FAB$^+$): *m*/*z* (%): 208 (100) $[Ni(dapi)Cl]^+$, 286–290 (36) superposition of $[Ni(dapi)_2-2H]^+$, $[Ni(dapi)_2-H]^+$, and $[Ni(dapi)_2]^+$, 323 (77) $[Ni(dapi)_2Cl]^+$, 379–384 (5) superposition of $[Ni_2(dapi)_2Cl-2H]^+$, $[Ni_2(dapi)_2Cl-H]^+$, 414–420 (16) superposition of $[Ni_2(dapi)_2Cl_2-2H]^+$, $[Ni_2(dapi)_2Cl_2-H]^+$, $[Ni_2(dapi)_2Cl_2]^+$, 453 (39) $[Ni_2(dapi)_2Cl_3]^+$.

[Cu(dapi)$_2$](NO$_3$)$_2$ (6(NO$_3$)$_2$): This complex was prepared from $Cu(NO_3)_2\cdot 3H_2O$ (105 mg, 0.43 mmol) and dapi·3HCl (195 mg, 0.87 mmol) by following the protocol for the preparation of the Ni complex $\mathbf{5}^{2+}$, yielding dark blue crystals suitable for single crystal X-ray analysis.

[Cu(dapi)Cl$_2$] (7): This complex was prepared from $CuCl_2\cdot 2H_2O$ (71 mg, 0.42 mmol) and dapi·3HCl (195 mg, 0.87 mmol), by following the protocol for the preparation of the Ni complex $\mathbf{5}^{2+}$. Yield: 47% of air-dried, blue crystals suitable for single crystal X-ray analysis. Elemental analysis calcd (%) for $C_5H_{13}Cl_2CuN_3$ (249.6): C 24.06, H 5.25, N 16.83; found C 24.34, H 5.21, N 16.74; MS (FAB$^+$): *m*/*z* (%): 178.0 (100) $[Cu(dapi)]^+$, 213.0 (40) $[Cu(dapi)Cl]^+$.

[{Cd(dapi)Cl$_2$}$_2$] (8): This complex was prepared from $CdCl_2\cdot 2H_2O$ (102 mg, 0.48 mmol) and dapi·3HCl (202 mg, 0.9 mmol) by following the protocol for the preparation of the Ni complex $\mathbf{5}^{2+}$. Yield: 18% of air-dried, colorless crystals suitable for single crystal X-ray analysis. Elemental analysis calcd (%) for $C_{10}H_{26}Cd_2Cl_4N_6$ (597.0): C 20.12, H 4.39, N 14.08; found C 19.96, H 4.39, N 13.85.

[Co(dapi)(CO$_3$)(NO$_2$)] (9): The ligand dapi·3HCl (1 g, 4.4 mmol) was dissolved in aqueous NaOH (1 mol dm^{-3}, 30 mL). A solution of $Na_3[Co(NO_2)_6]$ (2.2 g, 5.5 mmol) in water (50 mL) was added dropwise. The color of the solution turned to brown and a solid precipitated. This was removed by filtration, and the clear solution was allowed to stand open to the air for one week. A small amount of reddish crystals deposited. They were collected, dried in air and analyzed by single crystal X-ray diffraction. Elemental analysis calcd (%) for $C_6H_{13}CoN_4O_5$ (280.1): C 25.73, H 4.68, N 20.00; found C 25.00, H 4.53, N 19.53; ^{1}H NMR (D_2O): $\delta = 3.19$ (m, 2H), 2.95 (d, $J = 12$ Hz, 2H), 2.56 (d, $J = 12$ Hz, 2H), 1.93 (m, 1H), 1.83 (m, 1H); ^{13}C NMR{^{1}H} (D_2O): $\delta = 57.6$, 52.3, 33.5.

[Ni(py$_2$dapi)Cl](ClO$_4$) (10ClO$_4$): A solution of $Ni(ClO_4)_2\cdot 6H_2O$ (66 mg, 0.18 mmol) in water (5 mL) was added to a solution of $py_2dapi\cdot 5HCl\cdot 3.5H_2O$ (100 mg, 0.18 mmol) in water (10 mL). The solution was heated to 60 °C for 5 min (color change to pink) and allowed to cool to room temperature. It was layered with EtOH and allowed to stand at 4 °C. A crop of pink crystals, suitable for single crystal X-ray analysis, was removed by filtration and dried in air. Elemental analysis calcd (%) for $C_{17}H_{23}Cl_2N_5NiO_4$ (491.0): C 41.58, H 4.72, N 14.26; found C 41.56, H 4.60, N 14.00.

[Ni(py$_3$dapi)](ClO$_4$)$_2$·H$_2$O (11(ClO$_4$)$_2$·H$_2$O): The protocol for the preparation of **10**(ClO_4) was used, yielding purple crystals, suitable for single crystal X-ray analysis. Elemental analysis calcd (%) for $C_{23}H_{30}Cl_2N_6NiO_9$ (664.1): C 41.60, H 4.55, N 12.65; found C 41.05, H 4.35, N 12.61.

Potentiometric measurements and calculations of equilibrium constants: Potentiometric titrations were carried out with a Metrohm 713 pH/mV meter and a Metrohm combined glass electrode with an internal Ag/AgCl reference. The sample solutions were titrated with 0.1 mol dm^{-3} KOH, by using a Metrohm 665 piston burette. The stability of the electrode was checked by two calibration titrations prior to, and after, each measurement. All titrations were performed at 25.0 °C under nitrogen (scrubbed with an aqueous solution of 0.1 mol dm^{-3} KCl or KNO_3) at an ionic strength of 0.1 mol dm^{-3} (KCl or KNO_3). The Ni-dapi system was investigated by a batch-method as reported previously.[24] All other titrations were performed continuously with a measuring time of 3 min per point (pK_a determinations), or 12 min per point (metal complexes). For the pK_a determination of the ligands, several alkalimetric titrations were carried out with analytically pure samples of the hydrochlorides (total concentration: 10^{-3} or 2×10^{-3} mol dm^{-3}). Solutions for the titration experiments of $[M(dapi)]^{2+}$ and $[M(dapi)_2]^{2+}$ were prepared by dissolving dapi·3HCl and the metal salt in a 1:1 or 1:2 molar ratio with total $M = 1.0\times10^{-3}$ or 0.5×10^{-3} mol dm^{-3}. The solutions were made up by using standardized aqueous stock solutions of dapi·3HCl, $Cd(NO_3)_2\cdot 4H_2O$, $CdCl_2\cdot 2H_2O$, $CoCl_2\cdot 6H_2O$, $CuCl_2\cdot 2H_2O$, $NiCl_2\cdot 6H_2O$, and $ZnCl_2$. All equilibrium constants were calculated as concentration quotients by using the computer programs SUPERQUAD and BEST.[47, 48] A value of 13.79 was used for pK_w.[10] The titration experiments of the metal complexes were evaluated with fixed values for the total concentrations of M, dapi, and H, and for the pK_a's of dapi (Table 2). Further details of the potentiometric measurements and data evaluation are summarized in Tables S4–S6 (Supporting Information).

Crystal structure determination:[49] Data were collected on the following diffractometers (monochromated $Mo_{K\alpha}$ radiation): Siemens P4 (H_3dapi[$ZnCl_4$]Cl, **1**$Cl_3\cdot 2H_2O$, **2**$Cl_3\cdot H_2O$), STOE IPDS (**3**[$ZnCl_4$]Cl, **4**[$ZnCl_4$]Cl, **6**$(NO_3)_2$, **7**, **8**, **11**$(ClO_4)_2\cdot H_2O$), Siemens SMART PLATFORM (**5**$Cl_2\cdot H_2O$), Siemens STADI 4 (**9**, **10**ClO_4). A compilation of crystallographic data is given in Tables 9 and 10. A low temperature

Table 9. Crystallographic data for **1**$Cl_3\cdot 2H_2O$, **2**$Cl_3\cdot H_2O$, **3**[$ZnCl_4$]Cl, **4**[$ZnCl_4$]Cl, **5**$Cl_2\cdot H_2O$, **6**$(NO_3)_2$.

	1$Cl_3\cdot 2H_2O$	**2**$Cl_3\cdot H_2O$	**3**[$ZnCl_4$]Cl	**4**[$ZnCl_4$]Cl	**5**$Cl_2\cdot H_2O$	**6**$(NO_3)_2$
formula	$C_{10}Cl_3CoH_{26}N_6O_2$	$C_{10}Cl_3CoH_{26}N_6O$	$C_{16}Cl_5CoH_{30}N_6O_2Zn$	$C_{14}Cl_5CoH_{28}N_6OZn$	$C_{10}Cl_2H_{26}N_6NiO$	$C_{10}CuH_{26}N_8O_6$
M_w	427.65	411.65	640.01	597.97	375.96	417.93
T [K]	293(2)	223(2)	293(2)	298(2)	243(2)	293(2)
crystal system	monoclinic	monoclinic	orthorhombic	monoclinic	monoclinic	monoclinic
space group	*C*2/*c*	$P2_1/c$	$Pna2_1$	$P2_1/c$	$P2_1/c$	$P2_1/n$
a [Å]	14.862(3)	12.918(5)	22.211(4)	9.783(2)	14.845(3)	9.213(1)
b [Å]	9.4942(12)	11.432(5)	9.144(2)	15.320(3)	8.886(2)	10.107(1)
c [Å]	13.323(2)	11.390(5)	11.959(2)	15.524(3)	12.959(2)	10.027(1)
β [°]	111.482(11)	90.863(11)	90	103.98(1)	99.352(8)	112.97(2)
V [Å^3]	1749.4(5)	1681.9(12)	2428.8(8)	2257.8(8)	1686.7(19)	859.7(2)
Z	4	4	4	4	4	2
ρ_{calcd} [g cm^{-3}]	1.624	1.626	1.750	1.759	1.481	1.615
μ [mm^{-1}]	1.454	1.504	2.247	2.407	1.472	1.318
transmission min/max	0.422/0.934	0.496/0.943	–	0.259/0.608	0.472/0.843	
crystal size [mm]	0.52×0.48×0.40	0.50×0.40×0.34	0.20×0.15×0.10	0.25×0.20×0.15	0.60×0.50×0.12	0.50×0.50×0.30
θ range [°]	2.60–24.99	2.38–24.99	1.83–24.06	1.90–24.04	1.39–26.38	3.25–24.22
hkl ranges	−17/0; −11/0; −14/15	−15/15; 0/13; 0/13	−25/25; −10/10; −12/12	−11/10; 0/17; 0/16	−18/13; −10/11; −15/16	−10/10; −11/11; −11/11
reflections measured	1603	2528	14903	13000	10161	4766
unique reflections	1541	2363	3639	3366	3443	1358
reflections observed [$I > 2\sigma(I)$]	1414	2055	3267	2657	2760	1204
parameters	103	190	280	355	184	155
R_1 [%][a]	2.7	4.6	3.1	4.1	8.1	4.4
wR_2 [%][b]	8.1	13.3	7.2	10.1	21.8	13.0

[a] For [$I > 2\sigma(I)$]. [b] For all data.

0947-6539/00/0615-2844 $ 17.50+.50/0 *Chem. Eur. J.* **2000**, *6*, No. 15

Table 10. Crystallographic data for $(H_3dapi)[ZnCl_4]Cl$, **7**, **8**, **9**, **10**ClO_4, and **11**$(ClO_4)_2 \cdot H_2O$.

	$(H_3dapi)[ZnCl_4]Cl$	**7**	**8**	**9**	**10**ClO_4	**11**$(ClO_4)_2 \cdot H_2O$
formula	$C_5Cl_5H_{16}N_3Zn$	$C_5Cl_2CuH_{13}N_3$	$C_5CdCl_2H_{13}N_3$	$C_6CoH_{13}N_4O_5$	$C_{17}Cl_2H_{23}N_5NiO_4$	$C_{23}Cl_2H_{30}N_6NiO_9$
M_w	360.83	249.62	298.49	280.13	491.01	664.14
T [K]	293(2)	293(2)	293(2)	293	293(2)	293(2)
crystal system	monoclinic	orthorhombic	monoclinic	monoclinic	monoclinic	orthorhombic
space group	$P2_1/n$	$Pbcm$	$P2_1/c$	$P2_1/m$	$P2_1/n$	$Pbca$
a [Å]	7.9886(10)	8.069(1)	9.154(2)	7.0860(10)	7.579(2)	8.903(2)
b [Å]	16.133(3)	9.340(1)	7.698(2)	10.219(2)	12.979(3)	17.217(3)
c [Å]	10.9387(12)	12.628(1)	13.813(3)	7.4020(10)	20.712(4)	35.180(7)
β [°]	110.163(9)	90	92.17(3)	112.86(3)	95.25(3)	90.00
V [Å^3]	1323.4(3)	951.7(2)	972.7(4)	493.89(14)	2028.8	5392.5(19)
Z	4	4	4	2	4	8
ρ_{calcd} [g cm^{-3}]	1.811	1.742	2.038	1.884	1.608	1.636
μ [mm^{-1}]	2.834	2.799	2.739	1.753	1.26	0.982
transmission min/max	0.259/0.608	0.422/0.934	0.472/0.843	0.86/0.99	0.799/0.999	–
crystal size [mm]	0.62 × 0.59 × 0.17	0.30 × 0.30 × 0.10	0.08 × 0.06 × 0.05	0.30 × 0.20 × 0.10	0.4 × 0.3 × 0.25	0.15 × 0.13 × 0.10
θ range [°]	4.08–25.24	3.34–24.07	2.95–28.17	2.99–22.49	1.85–22.49	2.32–24.16
hkl ranges	−9/9; −19/19; −13/13	−9/9; −10/10; −14/14	−11/12; −10/10; −18/18	−7/7; 0/11; 0/7	−8/8; 0/13; 0/22	−9/9; −19/18; −40/40
reflections measured	9969	4997	9068	688	2802	26609
unique reflections	2387	781	2349	688	2654	4086
reflections observed [$I > 2\sigma(I)$]	1979	684	2144	656	2340	2734
parameters	173	77	100	82	274	397
R_1 [%][a]	2.3	3.1	3.2	2.1	3.6	4.8
wR_2 [%][b]	4.9	8.8	8.6	5.3	9.8	13.0

[a] For [$I > 2\sigma(I)$]. [b] For all data.

measurement was performed for **2**$Cl_3 \cdot H_2O$ [223(2) K] and for **5**$Cl_2 \cdot H_2O$ [243(2) K]. The data of all other compounds were collected at ambient temperature. Monitoring of standard reflections of $H_3dapi[ZnCl_4]Cl$, **1**$Cl_3 \cdot 2H_2O$, **2**$Cl_3 \cdot H_2O$, **9**, and **10**ClO_4 during data collection indicated no significant crystal decay ($\leq 3\%$). All data sets were corrected for Lorentz and polarization effects. An absorption correction was applied to the data of $H_3dapi[ZnCl_4]Cl$, **1**$Cl_3 \cdot 2H_2O$, **2**$Cl_3 \cdot H_2O$, **4**$[ZnCl_4]Cl$, **5**$Cl_2 \cdot H_2O$, **7**, **8**, **9**, and **10**ClO_4. Corresponding transmission coefficients T_{min} and T_{max} are listed in Tables 9 and 10. All structures were solved by Direct Methods[50] and refined by full-matrix least squares calculations[51] on F^2. All non-hydrogen atoms were refined in the anisotropic mode. The hydrogen atoms of **4**$[ZnCl_4]Cl$, **6**$(NO_3)_2$, and **7** were all located in a difference Fourier map and refined with fixed isotropic displacement parameters of 0.080 Å^2. The H(-N) hydrogen atoms of $H_3dapi[ZnCl_4]Cl$ and **10**ClO_4 were located and refined with variable isotropic displacement parameters. All other hydrogen atoms were placed at calculated positions (riding model, fixed isotropic displacement parameters with $U_{iso} = 1.5\ U_{eq}$ of the corresponding heavy atom). A disorder problem was encountered for **4**$[ZnCl_4]Cl$ and **11**$(ClO_4)_2 \cdot H_2O$. In the structure of **4**$[ZnCl_4]Cl$, two Cl atoms of the $ZnCl_4^{2-}$ counter ion are distributed over two sites with an occupancy of each 50%. This disorder disappeared if the refinement was performed in the acentric space group $P2_1$ [absolute structure parameter:[52] 0.12(4)]. However, inspection of the structure clearly revealed the presence of a glide plane for the complex cations, the Zn positions of the $[ZnCl_4]^{2-}$ anions, and the Cl^- counter ions, and the structure was therefore refined in the centrosymmetric space group $P2_1/c$. In the structure of **11**$(ClO_4)_2 \cdot H_2O$, the oxygen positions of both perchlorate ions are disordered. They were modeled by using a total of five (Cl1) or six (Cl2) oxygen positions with corresponding partial occupancies.

Molecular modeling calculations: These were carried out by using the commercially available program MOMEC97.[53] A validation of this force field for Co^{III}-hexaamine complexes is given in ref. [54]. The additional parameters required for the modeling of the coordinated methylideneimino groups were derived from a total of eight related Co^{III} complexes for which crystal structure data were available.[55] The parameters were adjusted systematically to achieve an optimal agreement between calculated and observed values of bond angles and bond lengths:[55] k_b (mdyn Å^{-1}), r_o (Å): Co^{III}-N_{imine} 1.75, 1.870; N_{imine}–C_{imine} 7.20, 1.290; k_θ (mdyn Å rad^{-2}), θ_o (rad): H-C_{imine}-H 0.45, 2.094; N_{imine}-Co^{III}-N_{imine} 0.05, 1.571; N-Co^{III}-N_{imine} 0.05, 1.571; Co^{III}-N_{imine}-C 0.20, 1.920; Co^{III}-N_{imine}-C_{imine} 0.40, 2.150; C_{imine}-N_{imine}-C 0.97, 2.094.

Acknowledgement

The cyclic voltammograms were measured by Alfred Lauer. Additional, independent CV measurements with **2**$^{2+/3+}$ and **5**$^{2+/3+}$ confirming the results presented in this paper have been carried out by I. Buder and Prof. Dr. G. Schwitzgebel (Saarbrücken). We thank Prof. Dr. M. Veith, Dr. V. Huch, A. Ries, and A. Zaschka (Saarbrücken), Prof. Dr. W. S. Sheldrick (Bochum), and Dr. P. Osvath (Melbourne) for support and helpful suggestions. Financial Support from Ciba Spezialitätenchemie Grenzach GmbH (J.W.P.), Deutsche Forschungsgemeinschaft (J.S.), Studienstiftung des deutschen Volkes (D.K.), and Fonds der Chemischen Industrie (K.H.) is gratefully acknowledged.

[1] D. A. House in *Comprehensive Coordination Chemistry*, *Vol. 2* (Ed.: G. Wilkinson) Pergamon, Oxford, **1987**, pp. 23–72.
[2] P. Paoletti, L. Fabbrizzi, R. Barbucci, *Inorg. Chim. Acta Rev.* **1973**, *7*, 43.
[3] P. Paoletti, R. Walser, A. Vacca, G. Schwarzenbach, *Helv. Chim. Acta* **1971**, *54*, 243.
[4] A. Zimmer, I. Müller, G. J. Reiss, A. Caneschi, D. Gatteschi, K. Hegetschweiler, *Eur. J. Inorg. Chem.* **1998**, 2079.
[5] a) A. Bianchi, M. Micheloni, P. Paoletti, *Coord. Chem. Rev.* **1991**, *110*, 17; b) A. E. Martell, R. D. Hancock, *Metal Complexes in Aqueous Solutions*, Plenum Press, New York, **1996**.
[6] P. Chaudhuri, K. Wieghardt, *Prog. Inorg. Chem.* **1987**, *35*, 329.
[7] a) R. A. D. Wentworth, J. J. Felten, *J. Am. Chem. Soc.* **1968**, *90*, 621; b) F. L. Urbach, J. E. Sarneski, L. J. Turner, D. H. Busch, *Inorg. Chem.* **1968**, *7*, 2169; c) R. A. D. Wentworth, *Inorg. Chem.* **1968**, *7*, 1030; d) R. F. Childers, R. A. D. Wentworth, *Inorg. Chem.* **1969**, *8*, 2218; e) R. F. Childers, R. A. D. Wentworth, L. J. Zompa, *Inorg. Chem.* **1971**, *10*, 302; f) L. Fabbrizzi, M. Micheloni, P. Paoletti, *Inorg. Chem.* **1976**, *15*, 1451; g) G. Schwarzenbach, H.-B. Bürgi, W. P. Jensen, G. A. Lawrance, L. Mønsted, A. M. Sargeson, *Inorg. Chem.* **1983**, *22*, 4029.
[8] L. Fabbrizzi, M. Micheloni, P. Paoletti, *J. Chem. Soc. Dalton Trans.* **1980**, 1055.
[9] J. E. Sarneski, A. T. McPhail, K. D. Onan, L. E. Erickson, C. N. Reilley, *J. Am. Chem. Soc.* **1977**, *99*, 7376.
[10] "Critically Selected Stability Constants of Metal Complexes", R. M. Smith, A. E. Martell, R. J. Motekaitis in *NIST Standard Reference*

Database 46 Version 5.0, NIST Standard Reference Data, Gaithersburg, MD 20899 (USA), **1998**.
[11] H. C. Wormser, *J. Pharm. Sci.* **1969**, *58*, 1038.
[12] a) H. Manohar, D. Schwarzenbach, *Helv. Chim. Acta* **1974**, *57*, 519; b) H. Manohar, D. Schwarzenbach, W. Iff, G. Schwarzenbach, *J. Coord. Chem.* **1979**, *8*, 213.
[13] a) D. Kuppert, G. Reiss, M. Wörle, U. Schilde, K. Hegetschweiler, *Abstracts of Papers*, 37th IUPAC Congress and 27th GDCh General Meeting, Berlin (Germany), **1999**, p 1072; b) D. Kuppert, G. Reiss, M. Wörle, U. Schilde, K. Hegetschweiler, Chimia, **1999**, *53*, 341.
[14] O. Siroky, PhD thesis, ETH Zürich (Switzerland) **1973**.
[15] Systematic names. dapi: *cis*-3,5-piperidinediamine; Me_5dapi: 1-*N,N,N′,N′*-pentamethyl-*cis*-3,5-piperidinediamine; $(Hhb)_2$dapi: 2-[({5-[(2-hydroxybenzyl)amino]-3-piperidinyl}amino)methyl]phenol; bz_2dapi: N^3,N^5-dibenzyl-*cis*-3,5-piperidinediamine; pydapi: N^3-(2-pyridinylmethyl)-*cis*-3,5-piperidinediamine; py_2dapi: N^3,N^5-bis(2-pyridinylmethyl)-*cis*-3,5-piperidinediamine; py_3dapi: N^3,N^5,1-tris(2-pyridinylmethyl)-*cis*-3,5-piperidinediamine; L^a: (6*R**,8*S**,15*R**,17*S**)-N^8,N^{17}-dimethylidene-3,12-dioxa-1,5,10,14-tetraazatricyclo-[13.3.1.$1^{6,10}$]icosane-8,17-diamine; L^b: (3*R**,5*S**)-N^3-methylidene-N^5-[({[5-(methyleneamino)-3-piperidinyl]amino}methoxy)methyl]-3,5-piperidinediamine.
[16] J. L. Sudmeier, C. N. Reilley, *Anal. Chem.* **1964**, *36*, 1698.
[17] P. Paoletti, M. Ciampolini, A. Vacca, *J. Phys. Chem*. **1963**, *67*, 1065.
[18] a) P. Comba, M. Maeder, L. Zipper, *Helv. Chim. Acta* **1989**, *72*, 1029; b) P. Comba, T. W. Hambley, L. Zipper, *Helv. Chim. Acta* **1988**, *71*, 1875.
[19] The two descriptors *endocyclic* and *exocyclic* refer to the location of the nitrogen atoms with respect to the piperidine ring throughout this work.
[20] P. Comba, A. F. Sickmüller, *Angew. Chem.* **1997**, *109*, 2089; *Angew. Chem. Int. Ed. Engl.* **1997**, *36*, 2006.
[21] P. Hendry, A. Ludi, *Adv. Inorg. Chem.* **1990**, *35*, 117.
[22] M. Melnik, M. Kabesova, L. Macaskova, C. E. Holloway, *J. Coord. Chem.* **1998**, *45*, 31.
[23] N. Arulsamy, J. Glerup, D. J. Hodgson, *Inorg. Chem.* **1994**, *33*, 3043.
[24] K. Hegetschweiler, V. Gramlich, M. Ghisletta, H. Samaras, *Inorg. Chem.* **1992**, *31*, 2341.
[25] A. Ringbom, *J. Chem. Educ.* **1958**, *35*, 282.
[26] P. Comba, A. F. Sickmüller, *Inorg. Chem.* **1997**, *36*, 4500.
[27] K. Hegetschweiler, M. Weber, V. Huch, M. Veith, H. W. Schmalle, A. Linden, R. J. Geue, P. Osvath, A. M. Sargeson, A. C. Willis, W. Angst, *Inorg. Chem.* **1997**, *36*, 4121.
[28] M. Ghisletta, L. Hausherr-Primo, K. Gajda-Schrantz, G. Machula, L. Nagy, H. W. Schmalle, G. Rihs, F. Endres, K. Hegetschweiler, *Inorg. Chem.* **1998**, *37*, 997.
[29] a) R. A. D. Wentworth, *Inorg. Chem.* **1971**, *10*, 2615; b) J. E. Bollinger, J. T. Mague, C. J. O'Connor, W. A. Banks, D. M. Roundhill, *J. Chem. Soc. Dalton Trans.* **1995**, 1677; c) J. E. Bollinger, J. T. Mague, W. A. Banks, A. J. Kastin, D. M. Roundhill, *Inorg. Chem.* **1995**, *34*, 2143; d) K. A. Hilfiker, M. W. Brechbiel, R. D. Rogers, R. P. Planalp, *Inorg. Chem.* **1997**, *36*, 4600; e) P. Caravan, C. Orvig, *Inorg. Chem.* **1997**, *36*, 236.
[30] a) K. Hegetschweiler, A. Egli, R. Alberto, H. W. Schmalle, *Inorg. Chem.* **1992**, *31*, 4027; b) J. Sander, K. Hegetschweiler, *Z. Kristallogr.* **2000**, *215*, 186.
[31] A. Kramer, R. Alberto, A. Egli, I. Novak-Hofer, K. Hegetschweiler, U. Abram, P. V. Bernhardt, P. A. Schubiger, *Bioconjugate Chem.* **1998**, *9*, 691.
[32] a) T. A. Kaden, *Top. Curr. Chem.* **1984**, *121*, 157; b) A. E. Martell, R. J. Motekaitis, M. J. Welch, *J. Chem. Soc. Chem. Commun.* **1990**, 1748; c) E. Cole, R. C. B. Copley, J. A. K. Howard, D. Parker, G. Ferguson, J. F. Gallagher, B. Kaitner, A. Harrison, L. Royle, *J. Chem. Soc. Dalton Trans.* **1994**, 1619.
[33] a) G. R. Weisman, D. J. Vachon, V. B. Johnson, D. A. Gronbeck, *J. Chem. Soc. Chem. Commun*. **1987**, 886; b) A. J. Blake, I. A. Fallis, R. O. Gould, S. Parsons, S. A. Ross, M. Schröder, *J. Chem. Soc. Chem. Commun.* **1994**, 2467; c) A. J. Blake, I. A. Fallis, S. Parsons, S. A. Ross, M. Schröder, *J. Chem. Soc. Dalton Trans.* **1996**, 525; d) C. Stockheim, L. Hoster, T. Weyhermüller, K. Wieghardt, B. Nuber, *J. Chem. Soc. Dalton Trans.* **1996**, 4409; e) D. Schulz, T. Weyhermüller, K. Wieghardt, B. Nuber, *Inorg. Chim. Acta* **1995**, *240*, 217; f) L. Cronin, B. Greener, S. P. Foxon, S. L. Heath, P. H. Walton, *Inorg. Chem.* **1997**, *36*, 2594.
[34] J. Dannacher, M. Hazenkamp, G. Schlingloff, F. Bachmann, K. Hegetschweiler, J. W. Pauly, WO 0026332, **2000** [*Chem. Abstr.* **2000**, *132*, 336140].
[35] K. Hegetschweiler, M. Weber, V. Huch, R. J. Geue, A. D. Rae, A. C. Willis, A. M. Sargeson, *Inorg. Chem.* **1998**, *37*, 6136.
[36] R. J. Geue, M. R. Snow, J. Springborg, A. J. Herlt, A. M. Sargeson, D. Taylor, *J. Chem. Soc. Chem. Commun.* **1976**, 285.
[37] D. Cremer, J. A. Pople, *J. Am. Chem. Soc.* **1975**, *97*, 1354.
[38] R. D. Hancock, *Acc. Chem. Res.* **1990**, *23*, 253.
[39] J. Gasteiger, O. Dammer, *Tetrahedron* **1978**, *34*, 2939.
[40] K. Hegetschweiler, R. D. Hancock, M. Ghisletta, T. Kradolfer, V. Gramlich, H. W. Schmalle, *Inorg. Chem.* **1993**, *32*, 5273.
[41] For these considerations, the non-hydrogen atomic positions obtained from the X-ray structural analyses {$[Co(tmca)_2]^{3+}$: ref. [27]; $\mathbf{1}^{3+}$ and $\mathbf{2}^{3+}$: this work} were used, and the H(-N) positions were calculated by using an N–H distance of 1.02 Å and an H-N-H angle of 110°.
[42] a) A. Bondi, *J. Phys. Chem.* **1964**, *68*, 441; b) S. S. Batsanov, *Russ. J. Inorg. Chem.* **1991**, *36*, 1694.
[43] A. G. Orpen, L. Brammer, F. H. Allen, O. Kennard, D. G. Watson, R. Taylor, *J. Chem. Soc. Dalton Trans.* **1989**, S1.
[44] M. Weber, D. Kuppert, K. Hegetschweiler, V. Gramlich, *Inorg. Chem.* **1999**, *38*, 859.
[45] J. Sander, U. Schilde, K. Hegetschweiler, unpublished results.
[46] R. Pizer, *Inorg. Chem.* **1984**, *23*, 3027.
[47] P. Gans, A. Sabatini, A. Vacca, *J. Chem. Soc. Dalton Trans.* **1985**, 1195.
[48] R. J. Motekaitis, A. E. Martell, *Can. J. Chem.* **1982**, *60*, 2403.
[49] Crystallographic data (excluding structure factors) for the structures reported in this paper have been deposited with the Cambridge Crystallographic Data Centre as supplementary publication nos. CCDC-137901 – CCDC-137912 for compounds $(H_3dapi)[ZnCl_4]Cl$, $\mathbf{1}Cl_3\cdot 2H_2O$, $\mathbf{2}Cl_3\cdot H_2O$, $\mathbf{3}[ZnCl_4]Cl$, $\mathbf{4}[ZnCl_4]Cl$, $\mathbf{5}Cl_2\cdot H_2O$, $\mathbf{6}(NO_3)_2$, **7**, **8**, **9**, $\mathbf{10}ClO_4$, $\mathbf{11}(ClO_4)_2\cdot H_2O$, respectively. Copies of the data can be obtained free of charge on application to CCDC, 12 Union Road, Cambridge CB21EZ, UK (fax: (+44)1223-336-033; e-mail: deposit@ccdc.cam.ac.uk)..
[50] G. M. Sheldrick, *SHELXS-86*, *Program for Crystal Structure Solution*, Göttingen, **1986**.
[51] G. M. Sheldrick, *SHELXL-93*, *Program for Crystal Structure Refinement*, Göttingen, **1993**.
[52] H. D. Flack, *Acta Crystallogr. Sect A* **1983**, *39*, 876.
[53] a) P. Comba, T. W. Hambley, N. Okon, G. Lauer, *MOMEC, A Molecular Modeling Package for Inorganic Compounds*, Heidelberg **1997**; b) P. Comba, T. W. Hambley, *Molecular Modeling of Inorganic Compounds*, VCH, Weinheim, **1995**.
[54] A. M. T. Bygott, A. M. Sargeson, *Inorg. Chem.* **1998**, *37*, 4795.
[55] D. Kuppert, Ph. D. Thesis, Universität Saarbrücken, **2000**.

Received: December 22, 1999 [F2201]

  0947-6539/00/0615-2846 $ 17.50+.50/0